Universal Journal of Catalysis Science
https://ojs.wiserpub.com/index.php/UJCS/

Review

H_2 as Clean Energy for Sustainable Future

Sovann Khan[1,2]* and Veasna Soum[1]

[1]Graduate School of Science, Royal University of Phnom Penh, Phnom Penh,12150 Cambodia.
[2]Current affiliation: International Institute for Carbon Neutral Energy Research (WPI-I[2]CNER), Kyushu University, Motooka 744, Nishi-ku, Fukuoka 819-0395, Japan.
E-mail:khan.sovann.455@m.kyushu-u.ac.jp

Received: 2 December 2022, **Revised:** 28 January 2023; **Accepted:** 6 March 2023

Abstract: H_2 is considered a clean fuel used in Fuel cell technology for electricity generation with zero greenhouse gas (GHG) emission. The demand for H_2 gas, typically for fuel cell electric vehicles (FCEVs), is increasing. However, the current H_2 production relies on natural gas and coals related to carbon oxide gas emission, which gives back to global warming concerns. Low-carbon production processes are needed to contribute to the United Nation's sustainable development goals (SDGs). Water-splitting reaction using photocatalysis or electrocatalysis is a promising method for producing H_2 from water, which is the earth-abundant resource. These H_2 production methods based on catalytic technologies require highly active catalyst materials with long-term stability. The development of non-conventional materials with consideration of nanostructure, multijunction, and defect engineering is explored to achieve highly active catalyst materials. This mini-review discusses a basic understanding of H_2 production from water-splitting reactions via photocatalysis and electrocatalysis, with outstanding examples of recent works reported. Last part, we provide a short study on the H_2 global market and policy in order to conclude the future direction of H_2 energy.

Keywords: Hydrogen energy, photocatalysis, electrocatalysis, fuel cell,

Nomenclature

Term	Description
GHG	Greenhouse gas
FCEV	Fuel cell electric vehicle
SDG	Sustainable development Goal
PEMFC	Proton exchange membrane fuel cell
AFC	Akaline fuel cell
PAFC	Phosphoric acid fuel cell
MCFC	Molten carbonate fuel cell
SOFC	Solid oxide fuel cell
HER	Hydrogen evolution reaction
OER	Oxygen evolution reaction
SHE	Solar-to-hydrogen-efficiency
AQE	Appearance quantum efficiency
PEC	Photoelectrochemical cell
PLDV	Passenger light-duty vehicle
DFT	Density functional theory

DOI: https://doi.org/10.37256/ujcs.1220232208

1. Introduction

Global warming, which causes the earth to become warmer yearly, is very concerning for life on earth. For a sustainable future enforced by the 2015 Paris Climate Accord, it was agreed that the remedy for environmental problems requires capping GHG emissions as soon as possible and holding global temperature rise below 2 ℃ in this century [1]. Global warming is commonly known as the effects of GHGs, which are mainly composed of CO_2 (76%), CH_4 (16%), NO_x (6%), and others (2%). A major GHG component is CO_2 gas, which originates from various sectors such as electricity and heat production (25%); agriculture, forestry, and other land use (24%); industry (21%); transportation (14%) and other (16%) [2]. Therefore, reducing CO_2 emissions is one of the targets for resolving global warming effects. The energy sector is one of the major CO_2-emitting sources, which come from the combustion of fossil fuels such as gasoline, coal, natural gas and so on [3,4]. Exploring alternative energy source, which is not harmful to the environment is very important.

In this context, hydrogen (H_2) gas is considered a clean energy source that emits zero CO_2. Hydrogen chemically reacts with oxygen through fuel cell technologies to produce electricity, water and small amount of heat [5]. Therefore, H_2 would be very potential candidate for the substitution of fossil fuels in the future, which contributes to SDGs of the United Nations [6]. Fuel cells produce electrical current that can be directly used as the power source for electric motors or illuminating a light bulb and a city. There are many kinds of fuel cell technologies, which are categorized based on their electrolytes and fuels such as:

(1) Proton exchange membrane fuel cell (PEMFC) or polymer-electrolyte membrane (PEM) fuel cell: PEMFC is operated at low temperature (< 100 ^oC) and high temperature (120-250 ^oC) [7]. PEMFC composes of solid polymer electrolytes and porous carbon combined with platinum-based catalysts as electrodes. Pure hydrogen is required to operate this fuel cell. Because it operates at low temperature, PEMFC enables to have quick start-up. High power density, lightweight, compact structures and better durability are major advantages of PEMFC. However, PEMFC needs noble metal catalysts (e.g., platinum), which results in a high-cost system [8]. Platinum catalyst is also sensitive to carbon monoxide poisoning. Therefore, highly pure fuel gas is needed, or additional reactors are required if fuel gas is from hydrocarbon fuels, which produce additional cost for the system. Primary applications of PEMFC are transportation (e.g., cars, buses and heavy-duty tracks) and some stationary applications [9].

(2) Alkaline fuel cell (AFC): AFC can operate at low temperature (<100 ^oC) [10]. Alkaline solution (e.g., KOH) is used as electrolytes in this fuel cell. Highly active catalysts such as platinum or silver are used as electrode materials at this low-temperature operation. Besides, non-precious metals (e.g., nickel) are also reported as electrodes for this fuel cell. However, non-precious metal catalyst needs higher temperature (200-250 ^oC [10]) to operate. At this high temperature, it requires a high-pressure system or highly concentrated electrolyte. The important advantages of AFC are low-temperature operation, high efficiency, and diverse choices of non-precious catalysts [11]. However, AFC is susceptible to CO_2 poisoning due to carbonate formation. Therefore, even small amount of CO_2 in the atmosphere can affect the cell performances and durability [12]. In addition, liquid electrolyte systems might give other problems such as wettability and corrosion. High power density of AFC is suitable in the W to kW-scale applications [13].

(3) Phosphoric acid fuel cell (PAFC): PAFC uses liquid phosphoric acid as an electrolyte, and operates at temperature range between 150 ^oC to 200 ^oC [14]. The common electrodes are porous carbon containing platinum catalyst. Because acid electrolyte cells are tolerant to CO_2, cells can operate with normal air and non-pure hydrogen fuel [10,15]. However, corrosion is among major problems that restrict construction materials' choices. Compared to PEMFC and AFC, PAFC has lower electricity efficiency. This poorer efficiency might be due to the low activity of air electrode caused by increased stability of formed peroxides in an acid environment . This cell is generally large and heavy. PAFC has been used as power plants [15].

(4) Molten carbonate fuel cell (MCFC): MCFC is the high-temperature fuel cell, which is operated at temperature higher than 600 ^oC [10,16]. Electrolyte composes of molten mixture of potassium carbonate and lithium carbonate to transport carbonate ions from cathode to anode. High-temperature operating allows non-precious metal catalysts (e.g., nickel) to be used in MCFC, resulting in reduced system's cost. Electricity conversion efficiency is higher than that of PAFC when it is coupled with turbine or waste heat. Unlike PEMFC, AFC and PAFC, MCFC enables to operate with pure H_2 fuel or H_2-contained fuels such as natural gas or biogas without external reformers [17]. However, major problem of this fuel cell is durability. Since MCFC operates at high temperature and corrosive electrolyte, cell components are easy to breakdown and reduced cell's life [16]. Exploring corrosion-resistant materials for cell's components is very important to improve the durability of cell. MCFC is used in gas and coal-based power plants for electrical utility, industrial and military applications [17].

(5) Solid fuel cell (SOFC): SOFC uses dense ceramic compounds as electrolytes, and operate at high temperature (900-1000 ^oC) [18]. Similar to MCFC, due to high-temperature operation, SOFC does not require noble metal catalysts, which produce low-cost systems. SOFC enables to reform internally the hydrocarbons, which allow to use not only hydrogen as fuel, but also other fuels such as CH_4 or other light hydrocarbons. Two types of

SOFC are classified based on their electrolytes . Ion-conducting SOFC is a conventional fuel cell, which its electrolyte is O^{2-} anion-permeable [19]. Due to low anion-conductivity at low temperature, ion-conducting SOFC is generally operated at high temperature. Recently, the development of SOFC operated at intermediate temperatures (600-800 ^{o}C) is a new trend of research to develop next generation of SOFCs in order to reduce the operational cost of system [20]. Proton-conducting SOFC, which its electrolyte enables to transport H^{+} ions from anode to cathode, is more promising in lower temperature operation (400-600 ^{o}C) [21]. SOFC highly tolerates to sulfur and carbon monoxides, which are among the major advantages over other cell types. However, high-temperature operation requires slow startup and low durability. SOFC might be not suitable for transportation applications.

To mitigate the CO_2 emission, the use of fuel cell in transportation sectors such cars, buses, trucks, trains, ships and etc. are in great interest. Among the above fuel cell types, PEMFCs are very promising in this application due to their portability and low-temperature operation [9]. A typical schematic of PEMFC is presented in Fig. 1(a). PEMFC mainly composes of anode, cathode and electrolyte. Different kinds of catalyst materials are deposited on substrate to form electrodes. H_2 is a common fuel used in this fuel cell. H_2 is catalytically ionized at anode and carries positive charge. Proton exchange membrane allows protons pass to cathode, while negative charged electrons provide current through wire, and utilized as electricity [22-24]. Fuel cells need H_2 as fuels and oxygen (possible extraction from air) to produce electricity, and release water molecules as waste. No CO_2 emission in these reactions, which enable them to be a perfect candidate for low-carbon energy production technology. Typically, the concept of using fuel cell as a power source for electric vehicle (EV) is demonstrated in Fig. 1(b). General Electric (GE) initially developed H_2-fuel cells used to power NASA's Gemini and Apollo space capsule in 1960s [25]. Later, the interest in using fuel cell in EV market started increasing. Nowadays, many EV manufacturers produce fuel cell electric vehicles (FCEVs). Fig.1(c) shows one of FCEV examples of Toyota Mirai, which is amongst the best-sold FCEV in the world, parked in front of Kyushu University hydrogen station, Japan.

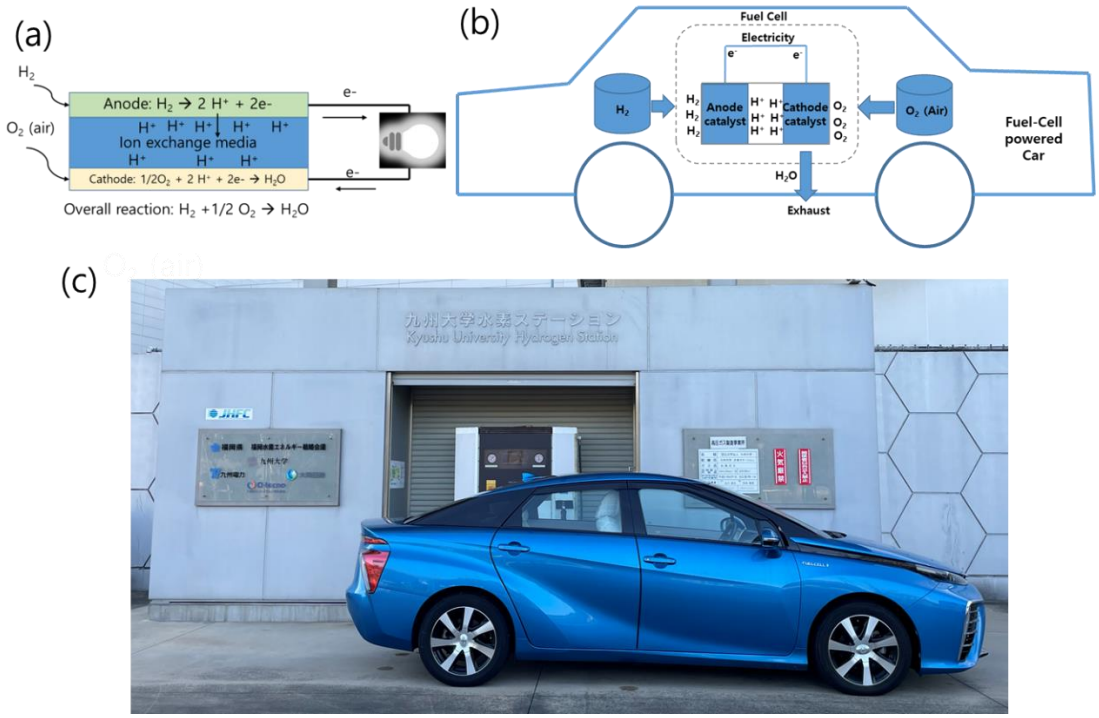

Fig. 1: (a) General schematics of PEMFC and (b) demonstrating concept for using fuel cell as power source of electric car, (c) Toyota Mirai powered by H_2 fuel cell parked in front of Kyushu University hydrogen station, Japan [image taken on 12 December 2022].

Although H_2-fuel cell technologies were ready to use for more than 60 years, they were not widely used as the common power sources due to the high price of H_2 and infrastructures [9]. H_2 is also the most plentiful element in the universe. H_2 can be produced from hydrogen-contained biomass, natural gas and water (H_2O). It has been challenging to extract H_2 gas from those natural compounds due to technological limits, typically for green H_2-production methods (e.g., water-splitting reaction) [26]. Until now, technologies used for H_2 production have been diversified. Typically, the advancement of nanotechnology enables various methods to produce H_2 more effectively and economically. Among production methods, water-splitting by photocatalysis and electrocatalysis is the most promising process in terms of environmental-friendly methods [27-30]. Water is an earth-abundant

resource and a green source for H_2 production. Water molecule is split to produce H_2 and O_2 gases via water-splitting reactions, and these gases are utilized for electricity generation releasing water molecules back via fuel cell. This process produces a clean energy cycle, which requires water, catalysts and fuel cells (see Fig. 2). Electricity is obtained and no GHG emission is involved. In this review, we highlight the basic understanding related to H_2 energy, including their production methods, H_2-to-electricity technologies (fuel cell) and the foreseen market trend. Typically, we select case studies from most recent reports as examples for intensive discussion of each process.

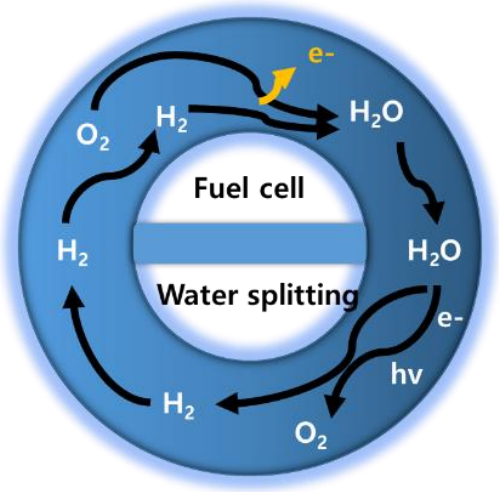

Fig. 2: A diagram of H_2 energy cycle from water.

2. H_2 production methods

2.1. Steam reforming methods

Hydrogen does not exist naturally as a pure gas. It is generally combined with other elements in the form of biomass, hydrocarbon, and water, which are used as the sources for H_2 productions [31]. Currently, major H_2 production is based on hydrocarbon fuels via steam reforming processes. For example, methane (CH_4) reforming via the following reactions [32-35]:

$$CH_4 + H_2O \rightarrow CO + 3H_2 \quad (1)$$

$$CO + H_2O \rightarrow CO_2 + H_2 \quad (2)$$

$$2CH_4 + O_2 + CO_2 \rightarrow 3H_2 + 3CO + H_2O \quad (3)$$

$$4CH_4 + O_2 + 2H_2O \rightarrow 10H_2 + 4CO \quad (4)$$

Steam reforming reactions are proceeded by catalyst and heat. In the current H_2 market, steam reforming methods are majorly used for the commercial production of H_2. However, these processes require higher energy consumption (high temperature) and release carbon oxide gases, which are among the green gases [36]. Therefore, low-carbon production processes are needed to replace these conventional methods.

2.2. Photocatalysis

After discovering the water-splitting reaction enabled by TiO_2 photocatalyst and light energy, photocatalytic H_2-generation became a clean and promising method, which requires only semiconductors and light energy (obtained from solar energy) [37]. When light energy, which equals or is higher than the bandgap energy of semiconductors, is radiated, electrons ($\mathbf{e}^-$) are excited to the conduction band (CB), leaving holes ($\mathbf{h}^+$) at the valence band (VB) (see Fig. 3(a)) [38,39]. Electrons and holes are active species in photocatalytic reactions. In photocatalytic water-splitting reaction, water molecules encounter oxidation reactions by holes to form oxygen gas and release protons (H^+) via equation (5). At CB, electrons process reduction reaction to form H_2 gas via equation (6). The overall reaction of this system produces oxygen and hydrogen gases from water molecules (equation (7)) [38,39].

$$H_2O + 2h^+ \rightarrow O_2 + 2H^+ \quad (5)$$

$$2H^+ + 2e^- \rightarrow H_2 \quad (6)$$

Total reaction:

$$H_2O \rightarrow 1/2O_2 + H_2 \quad (7)$$

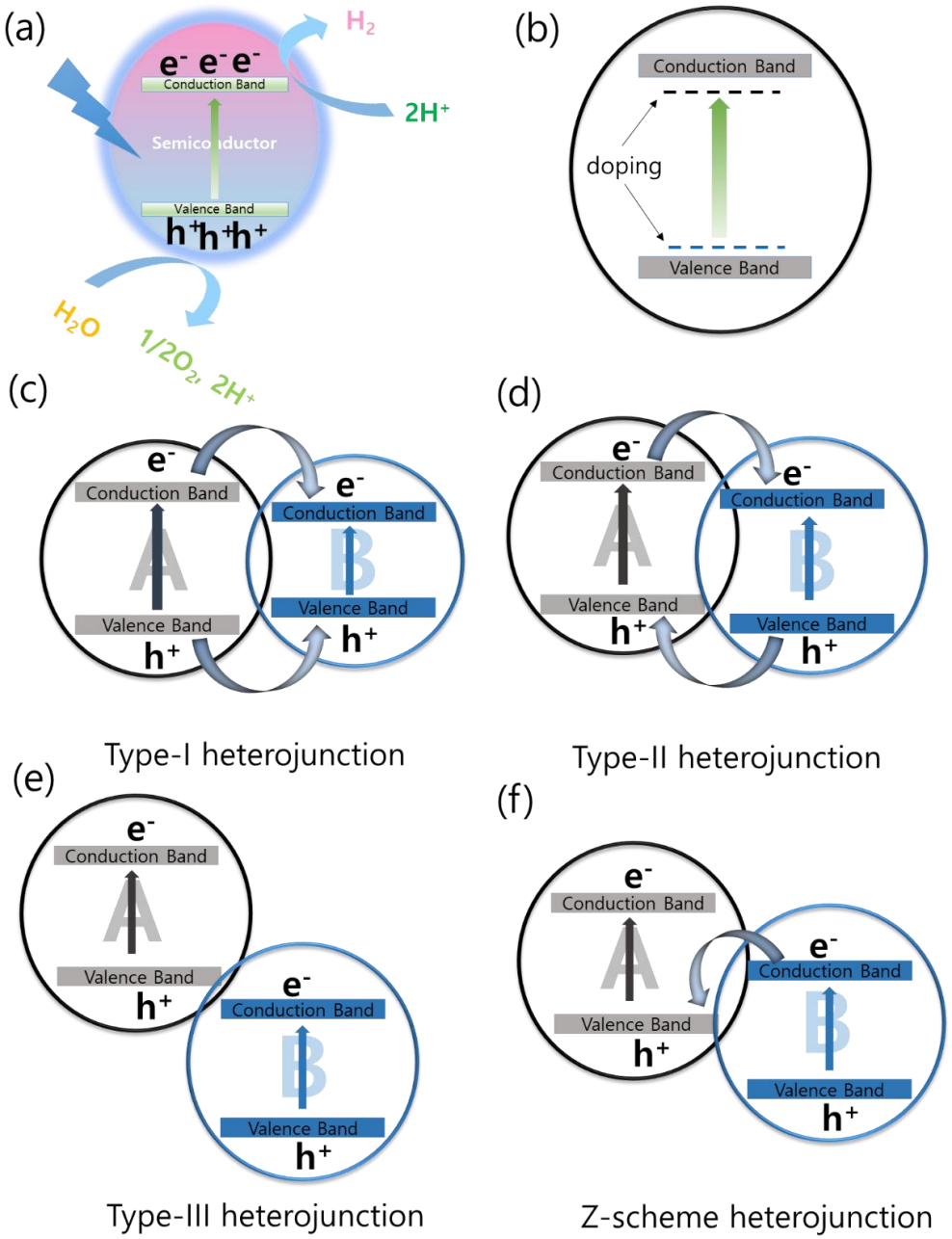

Fig. 3: (a) Schematics of photocatalytic water-spitting reaction by a semiconductor, (b) doping effects and (c)~(f) types of heterojunctions.

Water-splitting reaction by photocatalysis is a promising method for clean H_2 production. This method generates zero CO_2 emission from earth-abundant raw materials (e.g., water). Light energy can be obtained from sunlight. The most challenging work in this process is developing active photocatalysts. So far, active photocatalysts were developed such as TiO_2, $SrTiO_3$, $KTaO_3$, WO_3, ZnS, MoS_2, CdS, C_3N_4 and etc. [40,41]. However, most highly active materials (e.g., TiO_2) have large bandgap that is activated by ultraviolet (UV) light, only. Because the solar spectrum contains only small fraction of UV light (<5%) [41,42], solar-to-hydrogen efficiency (SHE) is very low to be utilized on industrial scales. Another barrier that limits the efficiency of the photocatalytic activities of those semiconductor materials is the rapid recombination rate between light-generated electrons and holes, which are active species in photocatalytic reactions. For example, the theoretical maximum SHE of anatase and rutile TiO_2 is only 1.3% and 2.2%, respectively [43]. Therefore, clear challenges must be addressed in order to realize the true potential of semiconductor photocatalysts in H_2-production industries. To overcome these issues, scientists have developed a number of resolutions for improving the efficiency of existing photocatalysts:

Defect engineering: native defects and impurity doping are utilized to improve photocatalysis under UV and visible light [29,44,45]. Native defects such as interstitials or vacancies are effectively utilized for improving

photocatalytic activities. To induce such kinds of defects, thermal treatment is the most common methods used [29,44]. We have induced different kinds of defects in brookite TiO_2 nanoparticles by annealing in different atmospheres [29]. We found that at light-reductive annealing, only oxygen vacancies (V_O^{2-}) were formed, while at an intermediate reductive atmosphere, Ti interstitial (Ti_i^{4+}) defects were preferentially formed. However, anti-site defects (Ti substituted O-site, Ti_O^{4+}) were dominant in a strong reductive atmosphere. And only Ti_i^{4+} defects were found to have beneficial effects for photocatalysis due to the formation of shallow-energy levels, which facilitated the charge transfer. In addition, the reduced state of titanium ions in TiO_2 such as Ti^{3+} species was well-known for enhanced visible-light photocatalysis [46-49]. In addition, native defects can induce by other methods such as chemical reduction [46,50,51], and plasma treatment [52-54].

Besides native defects, impurity doping is also conventionally used to enhance visible-light absorption of semiconductor photocatalysts by creating energy levels below the CB or upper the VB, which results in reduced bandgap energy (see Fig. 3(b)). Metal ions (e.g., Cr, Nb, W, Ce, Mn, Cu, Co, Ni and Fe [55-60]) are reported as dopants in various semiconductor photocatalysts. For example, W-doping has been successfully used to improve the photocatalytic activity of TiO_2 under visible light radiation [61]. Bandgap reduction originates from *d*-orbital state of W^{6+} creating mid-gap energy level below the CB of TiO_2. Typically, W^{6+}-doping in rutile phase reduces bandgap of TiO_2 more significantly than that in anatase one [61]. Cr ion is another dopant candidate, which effectively used to enhance visible light utilization of TiO_2 photocatalyst due to its strong interaction between of the Cr–O–Ti bond [62,63]. Doping Cr ions induce substantial amount of Ti^{3+}, which might account for the improving visible light photocatalysis [64]. The Cr^{6+} species is considered as the most active species in the Cr-doped TiO_2, because the synchronization of Cr^{6+} and TiO_2 is processed by the $Cr^{6+} = O^{2-} \rightarrow Cr^{5+}–O^{1-}$ route, which is responsible for the visible light photocatalytic reaction [65-69]. Besides metal doping, non-metal elements (e.g., N, C, S, P, B, F and I [70-75]) are also used to modify VB of semiconductor photocatalysts for reducing bandgap energy. In difference from metal doping, non-metal (anion) doping does not act as charge carriers and recombination centers, which do not produce drawback on photocatalysis. N-doping is one the well-known anion dopants for enhancing photocatalytic activity of semiconductors (e.g., TiO_2 [76,77], ZnO [78,79], ZnS [80,81]) in both visible and UV light. N-doped TiO_2 has been extensively investigated for effective visible-light photocatalysis. It is reported that visible light photocatalytic activity of N-doped TiO_2 influences by N-doping concentrations and doping sites. The dominant factor for the enhanced photocatalytic activities under visible light should be due to the reduced band gap energy of TiO_2 by incorporating N atoms into the TiO_2 lattice, resulting in the alteration of the electronic band structure. The N doping creates a mid-gap energy state of N *2p* formed above the O *2p* VB and narrows the band gap of TiO_2 from 3.07 to 2.47 eV [82].

2) heterojunction: constructing heterostructure with two or more materials/phases, which have perfect band alignment for charge-transfers, is used to separate photo-excited electron-hole pairs resulting in elongation of the lifetime of active species for chemical reactions [27,83,84]. Major heterojunctions of semiconductor photocatalysts are mainly categorized into four types: Type-I, Type-II, Type-III and Z-scheme heterojunction (see Fig. 3(c)~(f)). For **Type-I heterojunction** (straddling gap), the VB of A-semiconductor is lower than that of B-semiconductor, while the CB of A-semiconductor is higher than B-semiconductor's. In this case, both electrons and holes transfer from A-semiconductor to B-semiconductor. In Type-I system, the separation of electron and hole is less pronounced. Type-I heterojunctions such as TiO_2-WO_3 [85,86], TiO_2-ZrO_2 [85,87,88], TiO_2-Fe_2O_3 [85,89,90], TiO_2-MoS_2 [85,91,92], TiO_2-$BiVO_4$ [85,93] and etc. are reported so far. **Type-II heterojunction** (staggered gap) composes of A-semiconductor, which its CB is higher than that of B-semiconductor, while VB of B-semiconductor is lower than A's. So, electrons flow from A-semiconductor to B-conductor, while holes move from B-semiconductor to A-semiconductor. In Type-II, the electron-hole pairs are effectively separated, which result in higher photocatalytic reactions. Many Type-II heterojunctioned materials have been reported such as TiO_2 anatase-rutile [61,94,95], TiO_2-ZnO [96,97], TiO_2-SnO_2 [98,99], $BiWO_6$-Ag_2O [100], TiO_2-CuO/Cu_2O [100-104], $BiVO_4$-WO_3 [105-108], $SrTiO_3$-TiO_2 [109,110] and etc. When the bandgap is not overlapped between A and B-semiconductor, it is called **Type-III heterojunction** (broken gap). Few materials such as WO_3-$GdCrO_3$ [111-113], InSb-InAs [114], Sc_2CF_2/Sc_2CO_2 [115] and others are reported as Type-III heterojunction. Charge transfer does not occur in this system, which is not significant for the electron-hole pair separation method. Defect/bandgap engineering can be used to enhance the charge transfer within this system [111-113,116]. **Z-scheme heterojunction** is formed with A-semiconductor, which its CB and VB are higher than those of B-semiconductor. Electrons at the CB of B-semiconductor recombine with holes at the VB of A-semiconductor. In this manner, holes accumulate at the VB of B-semiconductor, while electrons accumulate at the CB of A-semiconductor. Number of highly active Z-scheme heterostructures have been developed such as, ZnS-ZnO [39,117-119], TiO_2-$_g$-C_3N_4 [120,121], TiO_2-CdS [122,123], ZnO-CdS [124,125], ZnO-$_g$-C_3N_4 [126,127], $CaIn_2S_4$-TiO_2 [128] and many others [120,129].

3) loading cocatalysts: cocatalysts are very promising for improving H_2 generation reactions. Loading cocatalysts such as noble metals (Pt, Rh, Ru, Pd [38,130-133]) and non-noble metals (Ni, Co, Cu [134-137]) is successfully utilized for enhanced H_2-production by photocatalysis [30]. It is well understood that loading metal

nanoparticles improves the H_2-production reaction over semiconductor photocatalysts based on two main factors: (1) reduction of the activation energy (overpotential) for the H_2-evolution reaction on the surface of a semiconductor and (2) improvement of the electron-hole separation [138]. To achieve high production of H_2 via water-splitting reaction, cocatalysts are considered as state-of-the-art for the synthesis of high-performance catalysts and catalyst compounds [38,131]. Multiple cocatalysts are successfully utilized for a high production rate of hydrogen. For example, Takata et al. synthesized Al-doped $SrTiO_3$ loading with Rh/Cr_2O_3 and CoOOH, and produced H_2 up to 96% of external quantum efficiency at 350-360 nm wavelengths. This is among the best photocatalyst compounds reported so far [139]. To harvest solar energy, the development of visible-light utilized photocatalyst is very hot topic and it is very challenging. Therefore, more complex structures of catalyst/catalyst compounds have been developed. We introduced a new multijunctional photocatalyst composed of C-doped ZnS-ZnO loading with Rh cocatalyst [45]. We consider nanostructure, doping and heterojunction into a single catalyst compound (see Fig. 4). First, ZnS/ethylenediamine nanosheet-complex is synthesized by solvothermal method. By controlling the annealing atmospheres (e.g., air, N_2 or O_2), ZnS, ZnO and ZnO-ZnS nanosheet composite can be obtained. Annealing in air at 500 ^oC for 1 h shows the best composite with the highest H_2 production from water-splitting reaction. More importantly, carbon decomposed from ethylenediamine is doped into both ZnS and ZnO. Density functional theory (DFT) calculation reveals that C-substitution for S as neutral charge (C_S^0) is dominant in ZnS. However, in ZnO, C-substitute for Zn is preferentially formed as a positive (C_{Zn}^{2+}) and neutral (C_{Zn}^0). C-doping is proven to reduce the bandgap of both ZnS and ZnO (see band diagram of Fig. 4(b)). After loading with Rh cocatalyst by photoreduction, the formed heterojunction of ZnS-ZnO/Rh ensures the effective electron-hole pair separation resulting in enhanced H_2-generation reaction. Nanosheet structure provides a large surface area for reaction and effective charge separation in photocatalysis. As a result, multijunctioned C-doped ZnS-ZnO/Rh photocatalyst enables to produce H_2 generation from broad-light spectrum of solar simulator (Fig. 4(c)~4(d)) [45].

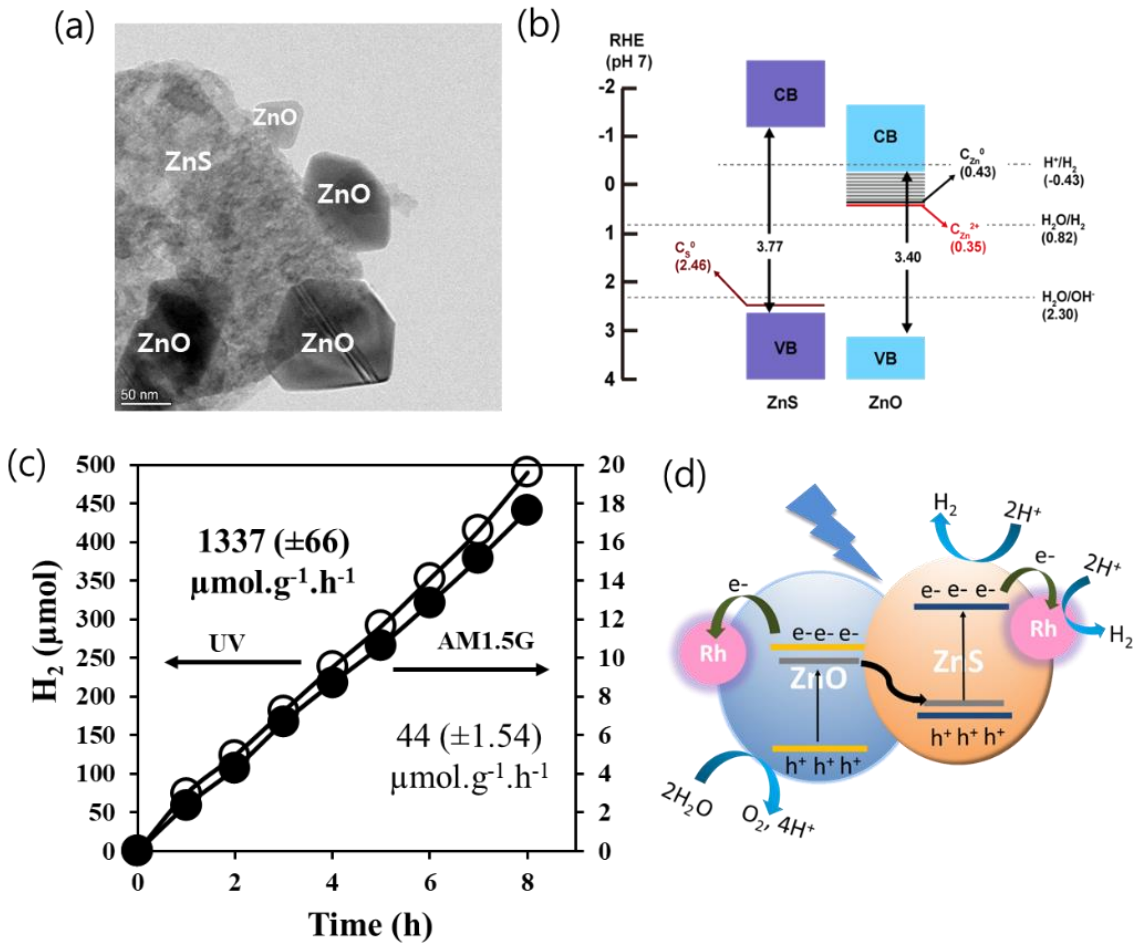

Fig. 4: Multijunctioned C-doped ZnS-ZnO/Rh photocatalyst (a) TEM image of ZnS-ZnO, (b) band diagram of C-doped ZnS and ZnO, (c) H_2-generation under 1-sun solar simulator and UV-light, (d) mechanism of enhanced visible-light photocatalytic H_2-generation [figures (b), (c), (d) are adapted from ref. [45] with permission from Elsevier, Copyright 2021].

Wang et al. developed photocatalyst sheets based on Z-scheme systems by combining a hydrogen evolution photocatalyst ($SrTiO_3$:La,Rh) and an oxygen evolution photocatalyst ($BiVO_4$:Mo), which enabled to harvest the sunlight for overall water-splitting reaction from pure water to produce oxygen and hydrogen gas, simutaneously [38]. These two photocatalyst sheets are embedded onto both sides of gold layers to form $SrTiO_3$:La, Rh/Au/$BiVO_4$:Mo as Z-scheme structure. When light is radiated, electrons are excited to CB and positive holes are at VB of both semiconductors. Holes at VB of $BiVO_4$:Mo oxidize water to form oxygen gas, and electrons transfer to Au nanoparticles. At the same time, electrons at CB of $SrTiO_3$:La, Rh reduce water to form hydrogen gas, while holes at VB of $SrTiO_3$:La, Rh transfer to Au nanoparticles. Therefore, overall water-splitting reaction is achieved by this system. To enhance activity of catalysts, Ru nanoparticles are deposited on the photocatalyst sheets by photodeposition. In addition, coating Ru particle's surface by Cr_2O_3 and amorphous TiO_2 layers is used to suppress the backward reactions, which allow the developed system maintain high activity under elevated pressures. In the preparation, annealing is an important process to remove impurity and reduce contact resistance, which facilitates the charge transfer within the system. This Z-scheme photocatalyst sheet showed excellent photocatalytic activity for pure water splitting with a solar-to-hydrogen energy conversion efficiency of 1.1% and appearance quantum efficiency (AQE) of > 30% at 419 nm [38].

2.3. Electrocatalysis

Water-splitting electrocatalysis for H_2 and O_2 production has been utilized for more 200 years. The electrolysis of water can be processed with minimum potential difference of 1.23 V in theory, which is equivalent to input energy of $\Delta G = 237.1$ kJ.mol^{-1}. However, overpotential is needed in practice to overcome the activation barrier of the reaction [140,141]. The general configuration of water electrocatalysis is represented in Fig. 5(a). Although water electrolysis was discovered since long time ago, this process was not yet applied for an industrial scale due to the need of electricity (energy) for processing. Recently, water electrolysis shows its promise in low-carbon processes for H_2 production [142]. Due to the advancement of material science and technologies, high-efficient electrodes have been developed, and they are on the ways of commercialization.

Overall-water splitting from pure water is hard to be proceeded due to limited self-ionization of water. Therefore, half-reactions of hydrogen evolution reaction (HER) and oxygen evolution reaction (OER) are generally operated in alkaline and acidic electrolyte:

In acidic electrolytes:

At anode (oxidation) $2H_2O_{(l)} \rightarrow O_{2(g)} + 4H^+_{(aq)} + 4e^-$ (8)

At cathode (reduction) $4H^+_{(aq)} + 4e^- \rightarrow 2H_{2(g)}$ (9)

In alkaline (basic):

At cathode (reduction) $4H_2O_{(l)} + 4e^- \rightarrow 2H_{2(g)} + 4OH^-_{(aq)}$ (10)

At anode (oxidation) $4OH^-_{(aq)} \rightarrow O_{2(g)} + 2H_2O_{(l)} + 4e^-$ (11)

Generally, in acidic reaction, noble metals are used as electrode materials such as Pt for HER and IrO_2 or RuO_2 for OER. Although noble metal-based catalysts produce high production yield in acidic medium, corrosion is the most important problem for long-term operation [143,144]. Challenges to synthesize catalysts, which enable to process in alkaline and neutral medium are among popular trends in current research. Typically, in HER, more sluggish in kinetics due to the slow water-dissociation reaction is widely known as factor limiting activity of hydrogen evolution from water electrolysis in alkaline and neutral medium. In the neutral/alkaline medium, low hydrogen adsorbed on active site of the catalyst's surface is the main reason of low hydrogen generation [145]. To overcome these issues, researchers have invented many strategies such as introducing transition metal hydroxide onto active catalysts [142,146], or surface/interface engineering to create more active site of catalysts [147,148]. Recently, Chen et al. introduced new method to synthesize highly active catalyst compound based on hydrogen spillover mechanism by integrating Ru nanoparticles onto the oxygen-deficient WO_{3-x} support [149]. Oxygen-deficient WO_{3-x} enables to store protons (a proton reservoir), and transfer to Ru nanoparticles during HER, enhancing HER reaction kinetics of Ru in neutral medium. HER of Ru/WO_{3-x} under neutral medium (1 M phosphate buffer solution) was achieved at low overpotential (~19 mV) to reach current density of 10 mA cm^{-2} with Tafel slope of 41 mV dec^{-1}. This HER activity was 24 times higher than that processed by commercial Ru/C electrode. This catalyst showed high stability up to 30 hours in neutral medium. A plausible mechanism of this enhanced HER activity is explained by hydrogen spillover mechanism. Under supplied cathodic potential, protons from electrolyte adsorb at oxygen-deficient WO_{3-x} to form H_xWO_{3-x}, and later transfer to Ru nanoparticles. Oxygen vacancies act as proton storage. When cathodic overpotential is increased, WO_{3-x}

dissociated water molecules to produce protons, which additionally spillover to Ru nanoparticles. Therefore, the rate-determining steps of HER in neutral medium from water dissociation to hydrogen recombination is changed, and enhanced HER kinetics [149].

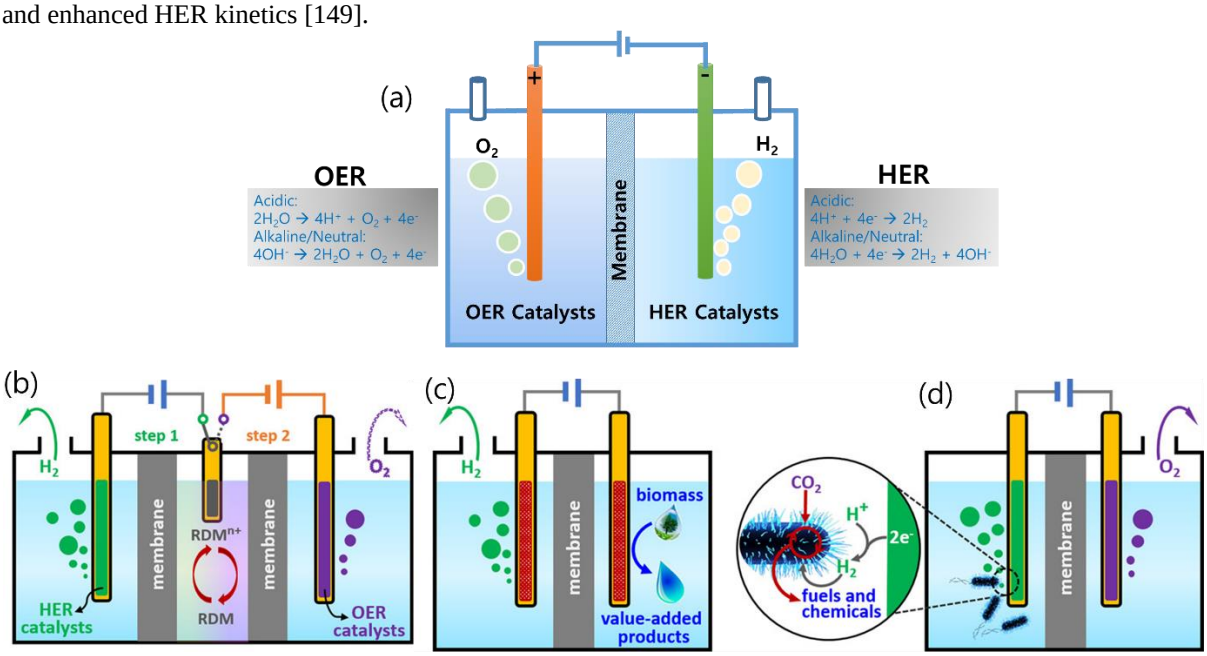

Fig. 5: (a) General reactor for water electrolysis, (b) decoupled water electrolysis, (c) hybrid water electrolysis, (d) tandem water electrolysis [figures (b), (c) and (d) are adapted from ref. [141] with permission from American Chemical Society, Copyright 2018].

In alkaline reaction, transition metal cocatalysts are always used [141]. Consideration of both performance and cost of the catalyst is very important for large-scale H_2 production via water electrolysis. Many efforts have been attempted to improve water electrolysis performance by developing active catalyst/catalyst compounds composed of functional and multicomponent structures. Besides, process operation and cell fabricating designs are also developed to be more advantageous than the conventional ones. To achieve overall water-splitting reaction, bifunctional electrocatalysts have been developed for both OER and HER in the same reaction electrolyte and cell. You and Sun successfully utilized CoP_x [150], Ni_2P [151], CoP_x embedded N-doped C-matrix (Co-P/NC) [152] and NiS_x [153] film obtaining by electrodeposition for active bifunctional catalyst for both OER and HER. However, this overall water-splitting proceeded by these materials were still unsatisfied. For targeting H_2 production, decoupled water electrolysis was developed by introducing redox mediators (see Fig. 5(b)). By shifting the operation of HER and OER, mixing H_2/O_2 and forming reactive oxygen species can be avoided. When a negative bias is applied, HER proceeds at the cathode and oxidizes the redox mediator at the counter electrode. When a positive bias is applied, OER processes at anode and reduces redox mediator to the original states together with oxygen evolution. Numbers of redox mediators were reported including acidic redox mediators (e.g., silicotungstic acid [154], phosphomolybdic acid [155], quinone derivatives [156]) and alkaline redox mediators (e.g., (ferrocenylmethyl)trimethylammonium chlorite (FcNCl) [157], $Na[Fe(CN)_6]$ [157], $Ni(OH)_2$ [158,159]). In some cases, oxygen is not the target product. Therefore, organic materials, which are easier to oxidize than water, are added into the reactor, which is called hybrid water electrolysis (Fig. 5(c)). There are number advantages of hybrid water electrolysis with biomass as oxidized substrate. Some organic biomasses can be oxidized at a lower bias applied, which results in higher current density at lower voltage input. Selected biomasses can be oxidized to form valued products [160]. Problem of O_2/H_2 mixture and reactive oxygen species formation can be avoided because no oxygen is produced. A high yield of H_2 production is achieved with separation-free process. Hybrid water electrolysis also shows its potential in pollutant decomposition for water treatment applications [161-164]. Rather than producing H_2 and store it for next use, this process is directly utilized hydrogen to produce valued products such as CH_4 and NH_3 by combining with biocatalysis called tandem water electrolysis (Fig. 5(d)). It is very innovative to create fuel from CO_2 coupled with water electrolysis and *Mathanosarcina barkeri* (*M. barkeri*) [165].

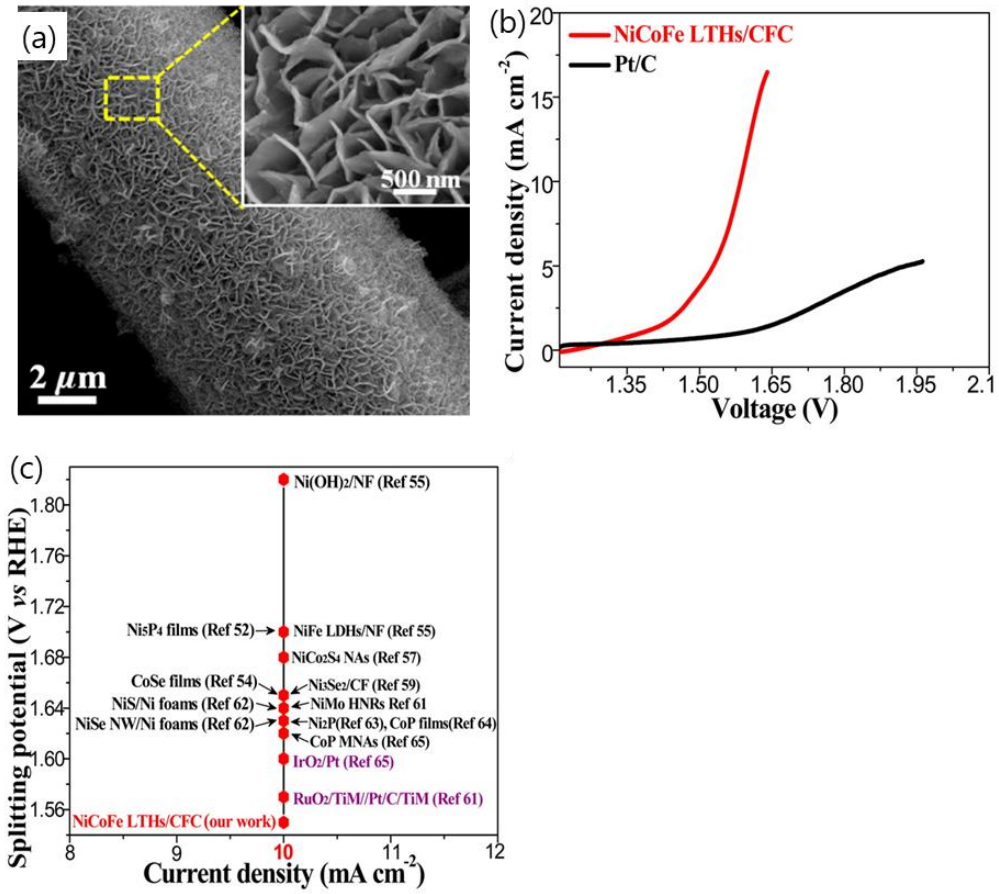

Fig. 6: NiCoFe layer triple hydroxide (LTHs) (a) SEM image of NiCoFe LTHs on carbon fiber cloth, (b) polarization curves of the overall water splitting using NiCoFe LTHs/CFC and Pt/C as functional electrocatalysts (same loading) in a two-electrode system, (c) comparisons of splitting potential of NiCoFe LTHs/CFC as bifunctional electrocatalysts with those of other bifunctional electrocatalysts at 20 mA cm^{-2} [adapted from ref. [166] with permission from American Chemical Society, Copyright 2016].

A typical example of nanostructured materials of NiCoFe layer triple hydroxide (LTHs) supported carbon fiber cloth (CFC) was developed for overall water-splitting electrolysis [166]. NiCoFe/CFC electrode was prepared by electrodeposition method. Well-defined nanostructure of ultrathin nanosheets (3~5 nm) wrapped uniformly on the CFC (Fig. 6(a)). Interlink of nanosheets creates network structures that provide space for transportation and diffusion of resultants and reactants, and enhanced fast transportation of electrons resulting in reduced resistance of NiCoFe/CFC electrocatalyst. OER operated in 1 M KOH showed a small onset potential ~1.45 V with an overpotential about 0.22 V and a small Tafel slope (~32 $mVdec^{-1}$). From the same reaction condition, NiCoFe/CFC afforded HER with a small onset potential ~0.180 V (overpotential ~0.20 V) and Tafel slope was ~70 $mVdec^{-1}$. With these excellent OER and HER electrocatalysis, NiCoFe/CFC enabled to perform overall water-splitting reaction in alkaline solution with onset potential of 1.51 V (Fig. 6(b)). With this small potential for overall water-splitting reaction, NiCoFe/CFC showed the best catalyst among reported catalysts in terms of both performance and durability (Fig. 6(c).

Besides metal-based catalysts/catalyst compounds, oxide perovskite materials (ABO_3, A: rare-earth alkaline metal ions, B: transition metal ions) have been considered as newly interested materials due to their high electrocatalytic activities and low cost [167-169]. Outstanding perovskite candidates have been developed for water electrolysis such as $SrCoO_3$ [170], $SrTiO_3$ [171], $LaNiO_3$ [172], $LaFeO_3$ [173] and etc. These perovskite oxides possess diverse physicochemical properties with doping foreign elements. It has been reported that both A and B-site doping affect the catalytic activities due to the change of electronic structures and defect formation. A-stie doping has been proved to have beneficial effects on OER/ORR activity by stabilizing the oxygen vacancies, subsequently influenced the electronic and chemical state of B-site ions [170,174-176]. Besides A-site doping, recent reports show that doping/co-doping at B-site exhibited excellent catalytic activity which attributes to a favourable balance of oxygen vacancy content, ion mobility and surface electron transfer [177]. To make more promising properties in term of both activity and stability, multi-components/structures were developed as composite structure between oxide perovskite and other materials (e.g., carbon). Bu et al., for example, synthesized heterostructures of $(PrBa_{0.5}Sr_{0.5})_{0.95}Co_{1.5}Fe_{0.5}O_{5-\delta}$ (PBSCF) and 3 dimensional structure (3D) of N-

doped graphene used as an electrocatalyst for OER and HER in alkaline medium [178]. N-doped graphene donates electrons to PBSCF, which enhances the OER by increasing the covalency between Co and lattice oxygen, and later, enhances HER by stabilizing H^* [178].

So far, the advancement of water electrolysis to produce green hydrogen from water becomes more practical for industrial scale production because various choices of highly active catalysts and reactors were well developed for all reaction media including acidic, alkaline, or neutral solution. Next challenge is to develop electrolyser, which can be operated effectively from saline water, directly. Due to the complex component of sea water, instability of electrolyser caused by electrode site effect reaction and corrosion is a big barrier for mass production of this green hydrogen. However, researchers are struggling to find the resolutions to solve this problem. Coating with chloride corrosion-tolerant materials such as polyanion coating can help with modest success [179,180]. Another way is to install pre-desalination process that can be used to avoid side-reaction and corrosion problem. However, this additional process provides additional cost to the system, which is not preferred for lost-cost production [181,182]. Recently, Xie et al. developed a membrane-based water electrolyser for hydrogen production from sea water with the integration of in situ water purification process, which enabled to operate at current density of 250 mA cm^{-2} for over 3200 hours [183]. In this system, in situ water purification process based on a self-driven phase transition mechanism could completely block the impurity ions (e.g., SO_4^{2-}, Cl^-, Mg^{2+} and etc.) to penetrate into electrolyser, which can address the side-reaction and corrosion problems [183]. This new discovery makes water electrolysis technology more promises for practical applications of hydrogen production from sea water.

2.4. Photoelectrochemical process

Photoelectrochemical cell (PEC) is a kind of photocatalytic devices, which utilize light to split water molecules to generate oxygens and hydrogens by photoelectrochemical reactions. The activity of semiconductor materials and the fabrication process of electrodes are key successes in high-performant PECs. Catalysts are deposited on a substrate to form electrodes (cathode and anode). Because the quality of films determines the performance of devices, development of deposition methods is very important. The common deposition methods used in PEC fabrication are solution process (e.g., spin-coating, deep-coating, doctor blade), chemical vapour deposition (CVD), laser/plasma-assisted deposition, electrodeposition and so on [43]. General setup of tandem PEC is represented in Fig. 7(a). Both cathode and anode are submerged into pure water or electrolytes. Light is radiated at both electrodes. As a n-type semiconductor, photogenerated holes accumulate on the surface of photoanode, and oxidize water molecules to form O_2. Photocathode, a p-type semiconductor, which conduction band edge is more negative than hydrogen evolution reaction potential, performs reduction reaction to form hydrogen gas [184]. From overall water-slitting reaction, oxygen gas is collected at anode side, while hydrogen gas is collected at cathode side. Photocathode materials (p-type semiconductor) such as GaP [185], InP [186], $GaInP_2$ [187], Si [188], WS_2 [189], $Cu(In,Ga)Se_2$ [190], Cu_2O [191], $CaFe_2O_4$ [192], Fe_2O_3 [193] and etc. are successfully developed for PEC's electrodes. In addition, photoanode materials (n-type semiconductor) are reported so far such as TiO_2 [194], WO_3 [195], α-Fe_2O_3 [196], $BiVO_4$ [197], $ZnFe_2O_4$ [198], β-Fe_2O_3 [199], Ta_3N_5 [200], TaON [201], and $SrTaO_2N$ [202]. Although PECs are very promising for clean H_2 production, research and development are ongoing to improve efficiency, durability, and cost reduction.

The following discussion is a typical example of efficient photocatalyst used for fabricating photoanode of PECs. To achieve high efficiency for solar-harvesting, photoanode materials need to have enough bandgap energy (>1.6 eV) to split the water, and not too big (<2.2 eV) to absorb the visible light from solar spectrum [184,203]. Corresponding to these criteria, Ta_3N_5 has suitable band position for water-spitting reaction and small bandgap (2.1 eV) for visible light absorption [204,205]. Li et al. fabricated vertically aligned Ta_3N_5 nanorod arrays using through-mask anodization method and utilized as a photoanode of high-performant PEC for water-splitting [203]. Fabricating process of Ta_3N_5 nanorod arrays is represented in Fig. 7(b). First, anodization of Al on Ta substrate forms the porous anodic alumina (PAA) mask, and then Ta_2O_5 nanorod arrays are formed by embedding into the nanochannels of PAA by Ta substrate anodizing. After selectively etching, Ta_2O_5 nanorod arrays standing on Ta substrate are obtained. Finally, Ta_2O_5 nanorods are converted to Ta_3N_5 nanorods by nitridation. Ta_3N_5 nanorod arrays have narrow size distribution (±10 nm) with a diameter of ~60 nm and length of ~600 nm (Fig. 7(c)). These Ta_3N_5 nanorod arrays are stable at high-temperature nitridation (1000 ^oC). After loading with IrO_2 cocatalyst, under AM1.5G simulated sunlight in a 0.5 M Na_2SO_4 solution (pH 13), the current density of sample annealed at 850 ^oC was 1.0 mA. Cm^{-2} at 1.23 V_{RHE}, which was less than that annealed at 1000 ^oC (~3.8 mA. Cm^{-2} at 1.23 V_{RHE}) (see Fig. 7(d)). At low-temperature nitridation (850 ^oC), polycrystalline Ta_3N_5 is formed as interlayer between Ta substrate and Ta_3N_5 nanorod arrays, which limit the electron transfer between catalyst and substrate due to poor electrical conductivity of polycrystalline Ta_3N_5. However, at high-temperature nitridation (1000 ^oC), polycrystalline Ta_3N_5 converts to metallic Ta_5N_6 and Ta_2N, which have better electrical conductivity. As a result, by nitridation at 1000 ^oC, Ta_3N_5 nanorod arrays produce high current density with a maximum incident photon-to-current conversion efficiency (IPCE) of 41.3% at 440 nm under 1.23 V_{RHE} [203].

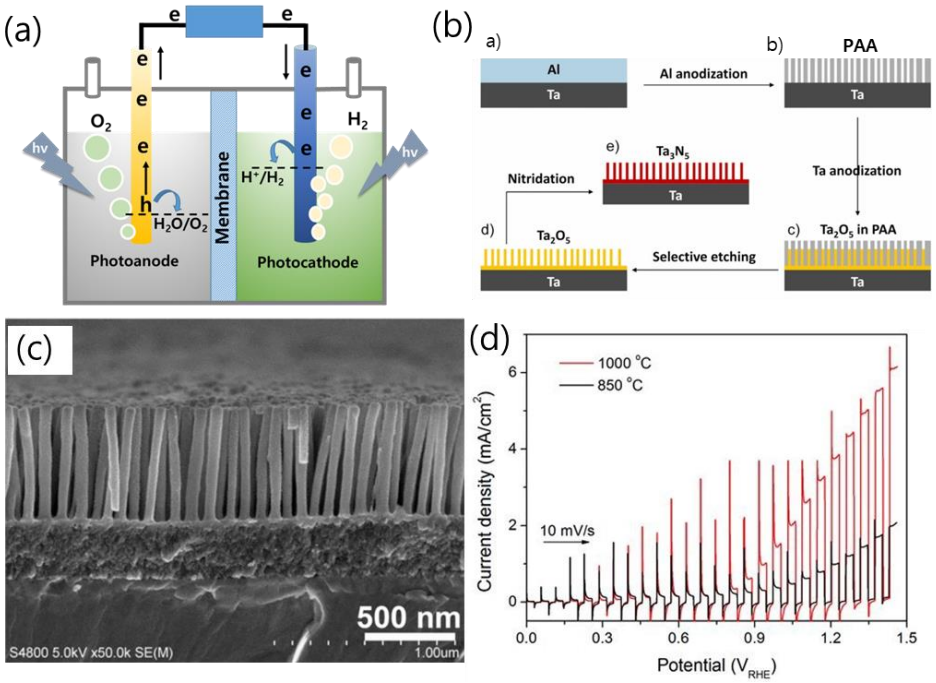

Fig. 7: (a) Schematics of a tandem PEC, (b) fabricating process of vertically aligned Ta_3N_5 nanorod array, (c) SEM images of Ta_3N_5 nanorod array, (d) current–potential curves of the IrO_2/Ta_3N_5 nanorod arrays nitrided at 850 °C and 1000 °C. [figures (b), (c) and (d) are adapted from ref. [203] with permission from John Wiley and Sons, Copyright 2013].

3. Global H_2 market and policy

Based on the sustainable development scenario, H_2 demand for the global market is expected to increase from 70.7 million tonnes per year in 2019 to 287 million tonnes per year in 2050 (see Fig. 8(a)) [206]. In 2050, some emerging sectors such as transportation, power, ammonia production and synfuel production are expected to take share of this hydrogen demand [206]. The current hydrogen demand is mostly used for oil refining and chemical production, and they are currently produced from natural gas and coal, and associated with CO_2 emissions [36]. However, hydrogen must be produced from low-carbon processes (LCP) for reliable and clean energy sources. Two major LCPs are utilized for commercial H_2 production: Combined conventional technologies with carbon capture and utilization or storage (CCUS) and water electrolysis. H_2 production by LCPs has been increasing drastically since 2020, and it is expected that H_2 production produced by LCPs will increase up to 7.92 million tonnes per year in 2030 (see Fig. 8(b)) [36]. Japan started operating the world's largest-class hydrogen production from water electrolysis using electricity from solar power in Fukushima in March 2020. This 10 MW project enables to produce 1200 Nm^3 of hydrogen per hour (rated power operation) [207]. Japan has targeted to make H_2 affordable in \$3/Kg by 2030 and \$2/Kg by 2050 through the Prime minister's initiative in "Basic Hydrogen Strategy" [208]. Danish government planned in May 2020 to build two energy islands, which can generate 4 GW of electricity and green hydrogen for various sectors such as shipping, aviation, industry and heavy transportation [209]. In June 2020, German Thyssenkrupp and Steag planned on a 500 MW hydrogen electrolysis plant to power steel production [210]. In December 2020, CWP Renewables, an Australian's green hydrogen project developers and partners launched the Green Hydrogen Catapult initiative in which 25 GW of renewable-based hydrogen would be produced by 2026, and the cost of hydrogen is expected to reduce to \$US2/Kg [211]. Recently, Bill Gates' Breakthrough Energy Ventures announced their leading funds of \$US22 million to Israeli-based H_2Pro for development of green hydrogen production, which their price is expected to \$US1/Kg. H_2Pro employs conventional electrochemical (E) and thermally-activated chemical (TAC), E-TAC, which water splitting efficiency can reach 95% [212]. Therefore, green production of H_2 would become a great interest for clean-energy businesses in the near future.

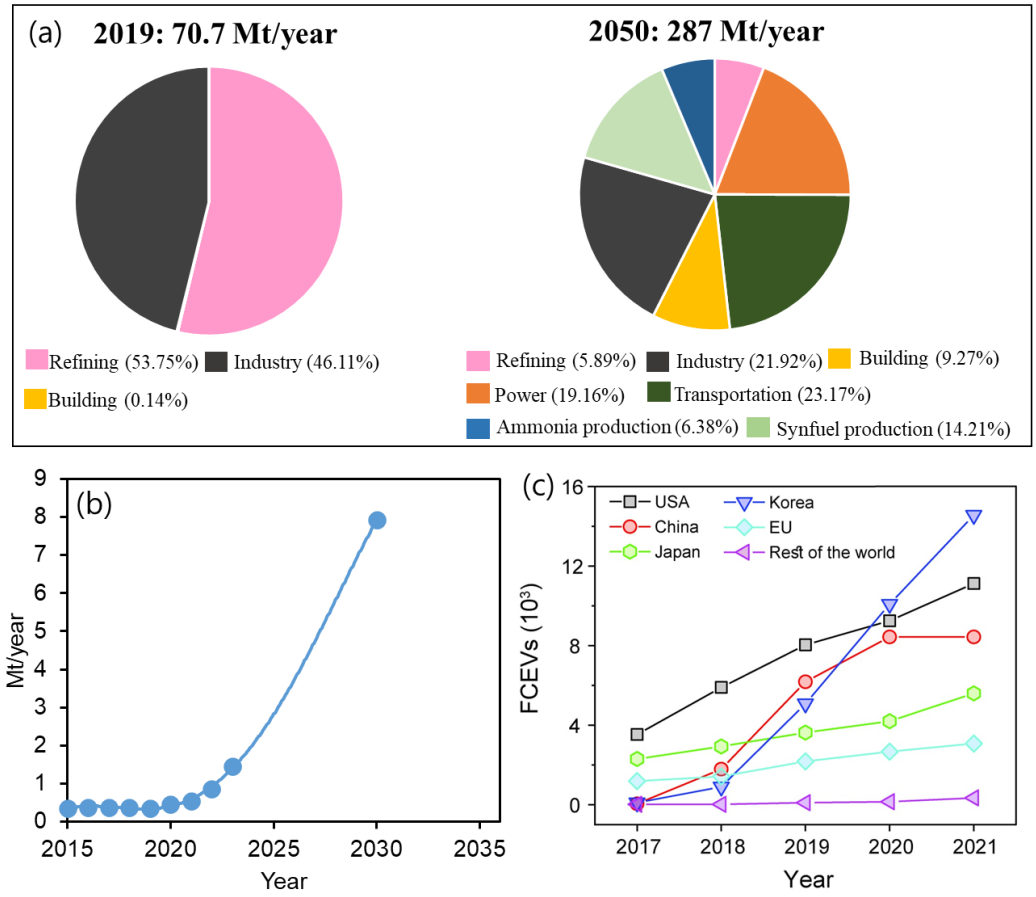

Fig. 8: (a) Global hydrogen demand by sector in the sustainable development scenario in 2019 and 2050 (IEA, 2022 [206]), (b) global hydrogen production by low-carbon methods (IEA, 2022 [36]), (c) fuel cell electric vehicle stock by region (IEA, 2022 [213])

One of the most important applications of H_2 is FCEV such as passenger light-duty vehicles (PLDVs), buses, trucks, ships, and aircrafts [214,215]. Among these FCEVs, PLDV is the most dominant stocks. Global FCEV stock was reported to 43140 units at the end of 2021 (IEA, 2022 [213]). Until 2019, USA was the world leader in FCEV stock followed by China, South Korea and Japan. It surprises the world that Asian countries such as Japan, Korea and China are expanding their FCEV stocks, drastically. The numbers of FCEVs in the USA in 2019 was 8040 units, while in China, Korea and Japan were 6180, 5080 and 3630 units, respectively (see Fig. 8(c)). South Korea's target stock is 200 000 and 2.9 million units in 2025 and 2040. Japan would increase to 200 000 and 800 000 units in 2025 and 2030. China's target is 50 000 and 1 million units in 2025 and 2030 [216]. Three popular FCEV models in global markets are Toyota's Mirai, Hyundai's Nexo and Honda Motor's Clarity Fuel Cell [217]. Nexo was the most-sold model FCEVs in 2019, mainly sold in South Korea's domestic market [218].

4. Summary and outlooks

H_2 is very promising energy source for the sustainable future of the earth. Through fuel cell technologies, H_2 can be utilized to produce electricity with zero CO_2 emission. H_2 FCEVs are emerging in global EV market, typically in Asian nations such as South Korea, Japan and China. Global demand for H_2 is increasing drastically. However, the current H_2 production has relied on conventional methods from natural gas and coal associated with CO_2 emissions. H_2 production from water-splitting reaction via photocatalysis and electrocatalysis is a green method and very promising for low-carbon society. In order to make this green technology as a true potential for our future energy, research and development need to be conducted to improve the current efficiency of catalysts and devices:

(1) *Photocatalysis/photoelectrochemical cell:* Highly active photocatalysts have been developed with efficiency upto > 96% under UV-light based on bandgap engineering and heterojunction. However, to harvest the solar energy, which is the unlimited energy on the earth, visible-light photocatalysts are needed. Currently, most high-performance photocatalyst and photocatalyst compounds are based on noble cocatalysts (e.g., Rh, Pt, Ru, Au …etc.). It leads to produce high production costs. It seems very a long way to go to develop highly active photocatalyst and photocatalyst compounds from non-precious elements.

(2) *Electrocatalysis:* Water electrolysis technology for H_2 production is vigorously developed. The operation of water electrolysis by excessive green electricity from wind, solar and hydropower is more and more feasible. A variety of electrocatalysts is available to use in the industrial scale. Therefore, number of commercial plants have been built, and are being built around the world. Soon, new emerging plants will enable water electrolysis as primary production for green hydrogen. However, it is not game over yet. To compete the conventional H_2 production, which mainly occupies the current H_2 market, research and development is further required to explore new catalysts and catalyst compounds, which are more actve, highely stable and cheaper.

Acknowledgments

S. Khan would like to thank to International Institute for Carbon-Neutral Energy Research, (WPI-I2CNER), Kyushu University for internal financial support for his research work. V. Soum was supported by Higher Education Improvement Project (HEIP) funded by the Royal Government of Cambodia through Ministry of Education, Youth and Sports (IDA Credit No. 6221-KH). V. Soum would like to thank to the Kansai-Asia Platform of Advanced Analytical Technologies (KAPLAT) Program, Japan Society for the Promotion of Science, and Prof. Toshiharu Teranishi and his group for hosting his research visit to the Institute for Chemical Research, Kyoto University. Authors also would like to thank Dr. Jin-Sung Park at Massachusetts Institute of Technology for useful discussion and reading our manuscript.

Conflict of interest

There is no conflict of interest for this study.

References

[1] United Nation, The Paris Agreement. 2015. https://unfccc.int/process-and-meetings/the-paris agreement/the-paris-agreement (Accessed date: 01 December 2022).
[2] United States Environmental Protection Agency, Global greenhouse gas emissions data. 2014. https://www.epa.gov/ghgemissions/global-greenhouse-gas-emissions-data (Accessed date: 01 December 2022).
[3] Ishaq H, Dincer I, Crawford C. A review on hydrogen production and utilization: Challenges and opportunities. *International Journal of Hydrogen Energy*. 2022;47(62):26238-64. https://doi.org/10.1016/j.ijhydene.2021.11.149
[4] Younas M, Shafique S, Hafeez A, Javed F, Rehman F. An overview of hydrogen production: current status, potential, and challenges. *Fuel*. 2022;316:123317. https://doi.org/10.1016/j.fuel.2022.123317
[5] Kirubakaran A, Jain S, Nema R. A review on fuel cell technologies and power electronic interface. *Renewable and Sustainable Energy Reviews*. 2009;13(9):2430-40. https://doi.org/10.1016/j.rser.2009.04.004
[6] United Nation. The 17 sustainable development goals (SDGs) to transform our world. 2021, doi:https://www.un.org/development/desa/disabilities/envision2030.html. [Accessed date: 01 December 2022].
[7] Haider R, Wen Y, Ma Z-F, Wilkinson DP, Zhang L, Yuan X, et al. High temperature proton exchange membrane fuel cells: progress in advanced materials and key technologies. *Chemical Society Reviews*. 2021;50(2):1138-87. 10.1039/D0CS00296H
[8] Fan L, Deng H, Zhang Y, Du Q, Leung DY, Wang Y, et al. Towards ultralow platinum loading proton exchange membrane fuel cells. *Energy & Environmental Science*. 2023. https://doi.org/10.1039/D2EE03169H
[9] Jiao K, Xuan J, Du Q, Bao Z, Xie B, Wang B, et al. Designing the next generation of proton-exchange membrane fuel cells. *Nature*. 2021;595(7867):361-9. 10.1038/s41586-021-03482-7
[10] Hirschenhofer JHS, D. B.; Engleman, R. R.; and Klett, M.G. . *Fuel cell handbook*. 4th, editor. USA: Parsons Corporation; 1998. p.1-5.
[11] Wagner E, Kohnke H-J. Another chance for classic afcs? Experimental investigation of a cost-efficient unitized regenerative alkaline fuel cell, using platinum-free gas diffusion electrodes. *Fuel Cells*. 2020;20(6):718-29. https://doi.org/10.1002/fuce.202000083
[12] Gülzow E. Alkaline fuel cells. *Fuel Cells*. 2004;4(4):251-5. https://doi.org/10.1002/fuce.200400042
[13] Kordesch K, Gsellmann J, Cifrain M, Voss S, Hacker V, Aronson RR, et al. Intermittent use of a low-cost alkaline fuel cell-hybrid system for electric vehicles. *Journal of Power Sources*. 1999;80(1):190-7. https://doi.org/10.1016/S0378-7753(98)00261-4

[14] Wilailak S, Yang J-H, Heo C-G, Kim K-S, Bang S-K, Seo I-H, et al. Thermo-economic analysis of phosphoric acid fuel-cell (PAFC) integrated with organic ranking cycle (ORC). *Energy*. 2021;220:119744. https://doi.org/10.1016/j.energy.2020.119744
[15] Sammes N, Bove R, Stahl K. Phosphoric acid fuel cells: Fundamentals and applications. *Current Opinion in Solid State and Materials Science*. 2004;8(5):372-8. https://doi.org/10.1016/j.cossms.2005.01.001
[16] Dicks AL. Molten carbonate fuel cells. *Current Opinion in Solid State and Materials Science*. 2004;8(5):379-83. https://doi.org/10.1016/j.cossms.2004.12.005
[17] Bischoff M, Huppmann G. Operating experience with a 250 kWel molten carbonate fuel cell (MCFC) power plant. *Journal of Power Sources*. 2002;105(2):216-21. https://doi.org/10.1016/S0378-7753(01)00942-9
[18] Simwonis D, Thülen H, Dias FJ, Naoumidis A, Stöver D. Properties of Ni/YSZ porous cermets for SOFC anode substrates prepared by tape casting and coat-mix® process. *Journal of Materials Processing Technology*. 1999;92-93:107-11. https://doi.org/10.1016/S0924-0136(99)00214-9
[19] Huang K, Wan J, Goodenough JB. Oxide-ion conducting ceramics for solid oxide fuel cells. *Journal of materials science*. 2001;36(5):1093-8. https://doi.org/10.1023/A:1004813305237
[20] Ju YW, Hyodo J, Inoishi A, Ida S, Tohei T, So YG, et al. Double columnar structure with a nanogradient composite for increased oxygen diffusivity and reduction activity. *Advanced Energy Materials*. 2014;4(17):1400783. https://doi.org/10.1002/aenm.201400783
[21] Lu Y, Mushtaq N, Yousaf Shah MAK, Irshad MS, Rauf S, Yousaf M, et al. A cobalt free triple charge conducting $Sm_{0.2}Ce_{0.8}O_{2-\delta}$-$Ba_{0.5}Sr_{0.5}Fe_{0.8}Sb_{0.2}O_{3-\delta}$ heterostructure composite cathode for protonic ceramic fuel cell. *Ceramics International*. 2023;49(2):2811-20. https://doi.org/10.1016/j.ceramint.2022.09.263
[22] Sazali N, Wan Salleh WN, Jamaludin AS, Mhd Razali MN. New perspectives on fuel cell technology: A brief review. *Membranes*. 2020;10(5):99. https://doi.org/10.3390/membranes10050099
[23] Wee J-H. Applications of proton exchange membrane fuel cell systems. *Renewable and Sustainable Energy Reviews*. 2007;11(8):1720-38. https://doi.org/10.1016/j.rser.2006.01.005
[24] Bose S, Kuila T, Nguyen TXH, Kim NH, Lau K-t, Lee JH. Polymer membranes for high temperature proton exchange membrane fuel cell: recent advances and challenges. *Progress in Polymer Science*. 2011;36(6):813-43. https://doi.org/10.1016/j.progpolymsci.2011.01.003
[25] Sharaf OZ, Orhan MF. An overview of fuel cell technology: Fundamentals and applications. *Renewable and Sustainable Energy Reviews*. 2014;32:810-53. https://doi.org/10.1016/j.rser.2014.01.012
[26] Staffell I, Scamman D, Abad AV, Balcombe P, Dodds PE, Ekins P, et al. The role of hydrogen and fuel cells in the global energy system. *Energy & Environmental Science*. 2019;12(2):463-91. https://doi.org/10.1039/C8EE01157E
[27] Khan S, Choi H, Kim D, Lee SY, Zhu Q, Zhang J, et al. Self-assembled heterojunction of metal sulfides for improved photocatalysis. *Chemical Engineering Journal*. 2020;395:125092. https://doi.org/10.1016/j.cej.2020.125092
[28] Khan S, Ikari H, Suzuki N, Nakata K, Terashima C, Fujishima A, et al. One-pot synthesis of anatase, rutile-decorated hydrogen titanate nanorods by yttrium doping for solar H_2 production. *ACS Omega*. 2020;5(36):23081-9. 10.1021/acsomega.0c02855
[29] Khan S, Je M, Kim D, Lee S, Cho S-H, Song T, et al. Mapping point defects of brookite TiO_2 for photocatalytic activity beyond anatase and P_{25}. *The Journal of Physical Chemistry C*. 2020;124(19):10376-84. https://doi.org/10.1021/acs.jpcc.0c02091
[30] Khan S, Kubota Y, Lei W, Suzuki N, Nakata K, Terashima C, et al. One-pot synthesis of (anatase/bronze-type)-TiO_2/carbon dot polymorphic structures and their photocatalytic activity for H_2 generation. *Applied Surface Science*. 2020;526:146650. https://doi.org/10.1016/j.apsusc.2020.146650
[31] Baykara SZ. Hydrogen: A brief overview on its sources, production and environmental impact. *International Journal of Hydrogen Energy*. 2018;43(23):10605-14. https://doi.org/10.1016/j.ijhydene.2018.02.022
[32] Haryanto A, Fernando S, Murali N, Adhikari S. Current status of hydrogen production techniques by steam reforming of ethanol: a review. *Energy & Fuels*. 2005;19(5):2098-106. 10.1021/ef0500538
[33] Siavashi M, Hosseini F, Bahrami HRT. A new design with preheating and layered porous ceramic for hydrogen production through methane steam reforming process. *Energy*. 2021;231:120952. https://doi.org/10.1016/j.energy.2021.120952
[34] Meloni E, Martino M, Ricca A, Palma V. Ultracompact methane steam reforming reactor based on microwaves susceptible structured catalysts for distributed hydrogen production. *International Journal of Hydrogen Energy*. 2021;46(26):13729-47. https://doi.org/10.1016/j.ijhydene.2020.06.299
[35] Chouhan K, Sinha S, Kumar S, Kumar S. Simulation of steam reforming of biogas in an industrial reformer for hydrogen production. *International Journal of Hydrogen Energy*. 2021. https://doi.org/10.1016/j.ijhydene.2021.05.152
[36] International energy agency (IEA), *Low-carbon hydrogen production, 2010-2030, historical, announced and in the sustainable development scenario, 2030, Paris* https://www.iea.org/data-and-

statistics/charts/low-carbon-hydrogen-production-2010-2030-historical-announced-and-in-the-sustainable-development-scenario-2030, IEA. License: CC BY *4.0*; 2022. [Accessed date: 01 December 2022].
[37] Fujishima A, Honda K. Electrochemical photolysis of water at a semiconductor electrode. *Nature*. 1972;238(5358):37-8. 10.1038/238037a0
[38] Wang Q, Hisatomi T, Jia Q, Tokudome H, Zhong M, Wang C, et al. Scalable water splitting on particulate photocatalyst sheets with a solar-to-hydrogen energy conversion efficiency exceeding 1%. *Nature materials*. 2016;15(6):611-5.
[39] Khan S, Poliukhova V, Tamir N, Park J, Suzuki N, Terashima C, et al. Dual function of rhodium photodeposition on ZnO/ZnS: Enhanced H_2 production and photocorrosion suppression in water. *International Journal of Hydrogen Energy*. 2023;48(26): 9713-9722-9722. https://doi.org/10.1016/j.ijhydene.2022.12.045
[40] Joy J, Mathew J, George SC. Nanomaterials for photoelectrochemical water splitting – review. *International Journal of Hydrogen Energy*. 2018;43(10):4804-17. https://doi.org/10.1016/j.ijhydene.2018.01.099
[41] Kudo A, Miseki Y. Heterogeneous photocatalyst materials for water splitting. *Chemical Society Reviews*. 2009;38(1):253-78. https://doi.org/10.1039/B800489G
[42] Chen X, Liu L, Huang F. Black titanium dioxide (TiO_2) nanomaterials. *Chemical Society Reviews*. 2015;44(7):1861-85. https://doi.org/10.1039/C4CS00330F
[43] Li J, Wu N. Semiconductor-based photocatalysts and photoelectrochemical cells for solar fuel generation: a review. *Catalysis Science & Technology*. 2015;5(3):1360-84. https://doi.org/10.1039/C4CY00974F
[44] Khan S, Cho H, Kim D, Han SS, Lee KH, Cho S-H, et al. Defect engineering toward strong photocatalysis of Nb-doped anatase TiO_2: Computational predictions and experimental verifications. *Applied Catalysis B: Environmental*. 2017;206:520-30. https://doi.org/10.1016/j.apcatb.2017.01.039
[45] Khan S, Je M, Ton NNT, Lei W, Taniike T, Yanagida S, et al. C-doped ZnS-ZnO/Rh nanosheets as multijunctioned photocatalysts for effective H_2 generation from pure water under solar simulating light. *Applied Catalysis B: Environmental*. 2021;297:120473. https://doi.org/10.1016/j.apcatb.2021.120473
[46] Xing M, Fang W, Nasir M, Ma Y, Zhang J, Anpo M. Self-doped Ti^{3+}-enhanced TiO_2 nanoparticles with a high-performance photocatalysis. *Journal of Catalysis*. 2013;297:236-43. https://doi.org/10.1016/j.jcat.2012.10.014
[47] Wang J, Zhang P, Li X, Zhu J, Li H. Synchronical pollutant degradation and H_2 production on a Ti^{3+}-doped TiO_2 visible photocatalyst with dominant (0 0 1) facets. *Applied Catalysis B: Environmental*. 2013;134:198-204. https://doi.org/10.1016/j.apcatb.2013.01.006
[48] Cao Y, Xing Z, Shen Y, Li Z, Wu X, Yan X, et al. Mesoporous black Ti^{3+}/N-TiO_2 spheres for efficient visible-light-driven photocatalytic performance. *Chemical Engineering Journal*. 2017;325:199-207. https://doi.org/10.1016/j.cej.2017.05.080
[49] Wang P, Jia C, Li J, Yang P. Ti^{3+}-doped TiO_2 (B)/anatase spheres prepared using thioglycolic acid towards super photocatalysis performance. *Journal of Alloys and Compounds*. 2019;780:660-70. https://doi.org/10.1016/j.jallcom.2018.11.398
[50] Xiu Z, Guo M, Zhao T, Pan K, Xing Z, Li Z, et al. Recent advances in Ti^{3+} self-doped nanostructured TiO_2 visible light photocatalysts for environmental and energy applications. *Chemical Engineering Journal*. 2020;382:123011. https://doi.org/10.1016/j.cej.2019.123011
[51] Fang W, Xing M, Zhang J. A new approach to prepare Ti^{3+} self-doped TiO_2 via $NaBH_4$ reduction and hydrochloric acid treatment. *Applied Catalysis B: Environmental*. 2014;160-161:240-6. https://doi.org/10.1016/j.apcatb.2014.05.031
[52] Yan Y, Han M, Konkin A, Koppe T, Wang D, Andreu T, et al. Slightly hydrogenated TiO_2 with enhanced photocatalytic performance. *Journal of Materials Chemistry A*. 2014;2(32):12708-16. https://doi.org/10.1039/C4TA02192D
[53] Nakamura I, Negishi N, Kutsuna S, Ihara T, Sugihara S, Takeuchi K. Role of oxygen vacancy in the plasma-treated TiO_2 photocatalyst with visible light activity for NO removal. *Journal of Molecular Catalysis A: Chemical*. 2000;161(1):205-12. https://doi.org/10.1016/S1381-1169(00)00362-9
[54] Li B, Zhao Z, Zhou Q, Meng B, Meng X, Qiu J. Highly efficient low-temperature plasma-assisted modification of TiO_2 nanosheets with exposed {001} facets for enhanced visible-light photocatalytic activity. *Chemistry–A European Journal*. 2014;20(45):14763-70. https://doi.org/10.1002/chem.201402664
[55] Venieri D, Fraggedaki A, Kostadima M, Chatzisymeon E, Binas V, Zachopoulos A, et al. Solar light and metal-doped TiO_2 to eliminate water-transmitted bacterial pathogens: Photocatalyst characterization and disinfection performance. *Applied Catalysis B: Environmental*. 2014;154-155:93-101. https://doi.org/10.1016/j.apcatb.2014.02.007

[56] Sun T, Fan J, Liu E, Liu L, Wang Y, Dai H, et al. Fe and Ni co-doped TiO_2 nanoparticles prepared by alcohol-thermal method: Application in hydrogen evolution by water splitting under visible light irradiation. *Powder Technology*. 2012;228:210-8. https://doi.org/10.1016/j.powtec.2012.05.018
[57] Ismael M. A review and recent advances in solar-to-hydrogen energy conversion based on photocatalytic water splitting over doped-TiO_2 nanoparticles. *Solar Energy*. 2020;211:522-46. https://doi.org/10.1016/j.solener.2020.09.073
[58] Gogoi D, Namdeo A, Golder AK, Peela NR. Ag-doped TiO_2 photocatalysts with effective charge transfer for highly efficient hydrogen production through water splitting. *International Journal of Hydrogen Energy*. 2020;45(4):2729-44. https://doi.org/10.1016/j.ijhydene.2019.11.127
[59] Iwase A, Kato H, Kudo A. The effect of alkaline earth metal ion dopants on photocatalytic water splitting by $NaTaO_3$ powder. *ChemSusChem*. 2009;2(9):873-7. https://doi.org/10.1002/cssc.200900160
[60] Jafari T, Moharreri E, Amin AS, Miao R, Song W, Suib SL. Photocatalytic water splitting—the untamed dream: A review of recent advances. *Molecules*. 2016;21(7):900. https://doi.org/10.3390/molecules21070900
[61] Choi H, Khan S, Choi J, Dinh DT, Lee SY, Paik U, et al. Synergetic control of band gap and structural transformation for optimizing TiO_2 photocatalysts. *Applied Catalysis B: Environmental*. 2017;210:513-21. https://doi.org/10.1016/j.apcatb.2017.04.020
[62] Inturi SNR, Boningari T, Suidan M, Smirniotis PG. Visible-light-induced photodegradation of gas phase acetonitrile using aerosol-made transition metal (V, Cr, Fe, Co, Mn, Mo, Ni, Cu, Y, Ce, and Zr) doped TiO_2. *Applied Catalysis B: Environmental*. 2014;144:333-42. https://doi.org/10.1016/j.apcatb.2013.07.032
[63] Inturi SNR, Boningari T, Suidan M, Smirniotis PG. Flame aerosol synthesized Cr incorporated TiO_2 for visible light photodegradation of gas phase acetonitrile. *The Journal of Physical Chemistry C*. 2014;118(1):231-42. https://doi.org/10.1021/jp404290g
[64] Chen X, Liu L, Yu PY, Mao SS. Increasing solar absorption for photocatalysis with black hydrogenated titanium dioxide nanocrystals. *Science*. 2011;331(6018):746-50. 10.1126/science.1200448
[65] Davydov L, Reddy EP, France P, Smirniotis PG. Transition-metal-substituted titania-loaded mcm-41 as photocatalysts for the degradation of aqueous organics in visible light. *Journal of Catalysis*. 2001;203(1):157-67. https://doi.org/10.1006/jcat.2001.3334
[66] Reddy EP, Sun B, Smirniotis PG. Transition metal modified TiO_2-loaded MCM-41 catalysts for visible- and UV-light driven photodegradation of aqueous organic pollutants. *The Journal of Physical Chemistry B*. 2004;108(44):17198-205. 10.1021/jp047419m
[67] Sun B, Reddy EP, Smirniotis PG. Effect of the Cr^{6+} concentration in Cr-incorporated TiO_2-loaded MCM-41 catalysts for visible light photocatalysis. *Applied Catalysis B: Environmental*. 2005;57(2):139-49. https://doi.org/10.1016/j.apcatb.2004.10.016
[68] Herrmann J-M. Fundamentals and misconceptions in photocatalysis. *Journal of Photochemistry and Photobiology A: Chemistry*. 2010;216(2):85-93. https://doi.org/10.1016/j.jphotochem.2010.05.015
[69] Sun B, Reddy EP, Smirniotis PG. TiO_2-loaded Cr-modified molecular sieves for 4-chlorophenol photodegradation under visible light. *Journal of Catalysis*. 2006;237(2):314-21. https://doi.org/10.1016/j.jcat.2005.10.028
[70] Devi LG, Kavitha R. A review on non metal ion doped titania for the photocatalytic degradation of organic pollutants under UV/solar light: Role of photogenerated charge carrier dynamics in enhancing the activity. *Applied Catalysis B: Environmental*. 2013;140-141:559-87. https://doi.org/10.1016/j.apcatb.2013.04.035
[71] Basavarajappa PS, Patil SB, Ganganagappa N, Reddy KR, Raghu AV, Reddy CV. Recent progress in metal-doped TiO_2, non-metal doped/codoped TiO_2 and TiO_2 nanostructured hybrids for enhanced photocatalysis. *International Journal of Hydrogen Energy*. 2020;45(13):7764-78. https://doi.org/10.1016/j.ijhydene.2019.07.241
[72] Marschall R, Wang L. Non-metal doping of transition metal oxides for visible-light photocatalysis. *Catalysis Today*. 2014;225:111-35. https://doi.org/10.1016/j.cattod.2013.10.088
[73] Ahamad T, Naushad M, Al-Saeedi SI, Almotairi S, Alshehri SM. Fabrication of MoS_2/ZnS embedded in N/S doped carbon for the photocatalytic degradation of pesticide. *Materials Letters*. 2020;263:127271. https://doi.org/10.1016/j.matlet.2019.127271
[74] Zhou Y, Chen G, Yu Y, Feng Y, Zheng Y, He F, et al. An efficient method to enhance the stability of sulphide semiconductor photocatalysts: a case study of N-doped ZnS. *Physical Chemistry Chemical Physics*. 2015;17(3):1870-6. https://doi.org/10.1039/C4CP03736G
[75] Cao L, Zhang B, Ou X, Wang C, Peng C, Zhang J. Synergistical coupling interconnected ZnS/SnS_2 nanoboxes with polypyrrole-derived N/S dual-doped carbon for boosting high-performance sodium storage. *Small*. 2019;15(9):1804861. https://doi.org/10.1002/smll.201804861

[76] Choi H, Shin D, Yeo BC, Song T, Han SS, Park N, et al. Simultaneously controllable doping sites and the activity of a W–N codoped TiO_2 photocatalyst. *ACS Catalysis*. 2016;6(5):2745-53. 10.1021/acscatal.6b00104
[77] Ansari SA, Khan MM, Ansari MO, Cho MH. Nitrogen-doped titanium dioxide (N-doped TiO_2) for visible light photocatalysis. *New Journal of Chemistry*. 2016;40(4):3000-9. https://doi.org/10.1039/C5NJ03478G
[78] Macías-Sánchez JJ, Hinojosa-Reyes L, Caballero-Quintero A, de la Cruz W, Ruiz-Ruiz E, Hernández-Ramírez A, et al. Synthesis of nitrogen-doped ZnO by sol–gel method: characterization and its application on visible photocatalytic degradation of 2,4-D and picloram herbicides. *Photochemical & Photobiological Sciences*. 2015;14(3):536-42. 10.1039/C4PP00273C
[79] Wang M, Ren F, Zhou J, Cai G, Cai L, Hu Y, et al. N doping to ZnO nanorods for photoelectrochemical water splitting under visible light: engineered impurity distribution and terraced band structure. *Scientific Reports*. 2015;5(1):12925. 10.1038/srep12925
[80] Jang JW, Choi SH, Jang JS, Lee JS, Cho S, Lee K-H. N-doped ZnS nanoparticles prepared through an inorganic−organic hybrid complex $ZnS{\cdot}(piperazine)_{0.5}$. *The Journal of Physical Chemistry C*. 2009;113(47):20445-51. 10.1021/jp907526e
[81] Xiong J, Wang X, Wu J, Han J, Lan Z, Fan J. In situ fabrication of N-doped ZnS/ZnO composition for enhanced visible-light photocatalytic H_2 evolution activity. *Molecules*. 2022;27(23):8544. https://doi.org/10.3390/molecules27238544
[82] Boningari T, Inturi SNR, Suidan M, Smirniotis PG. Novel one-step synthesis of nitrogen-doped TiO_2 by flame aerosol technique for visible-light photocatalysis: effect of synthesis parameters and secondary nitrogen (N) source. *Chemical Engineering Journal*. 2018;350:324-34. https://doi.org/10.1016/j.cej.2018.05.122
[83] Wang H, Zhang L, Chen Z, Hu J, Li S, Wang Z, et al. Semiconductor heterojunction photocatalysts: design, construction, and photocatalytic performances. *Chemical Society Reviews*. 2014;43(15):5234-44. https://doi.org/10.1039/C4CS00126E
[84] Low J, Yu J, Jaroniec M, Wageh S, Al-Ghamdi AA. Heterojunction photocatalysts. *Advanced Materials*. 2017;29(20):1601694. https://doi.org/10.1002/adma.201601694
[85] Marschall R. Semiconductor composites: Strategies for enhancing charge carrier separation to improve photocatalytic activity. *Advanced Functional Materials*. 2014;24(17):2421-40. https://doi.org/10.1002/adfm.201303214
[86] Karácsonyi É, Baia L, Dombi A, Danciu V, Mogyorósi K, Pop L, et al. The photocatalytic activity of TiO_2/WO_3/noble metal (Au or Pt) nanoarchitectures obtained by selective photodeposition. *Catalysis Today*. 2013;208:19-27. https://doi.org/10.1016/j.cattod.2012.09.038
[87] Kambur A, Pozan GS, Boz I. Preparation, characterization and photocatalytic activity of TiO_2–ZrO_2 binary oxide nanoparticles. *Applied Catalysis B: Environmental*. 2012;115:149-58. https://doi.org/10.1016/j.apcatb.2011.12.012
[88] Siedl N, Elser MJ, Bernardi J, Diwald O. Functional interfaces in pure and blended oxide nanoparticle networks: recombination versus separation of photogenerated charges. *The Journal of Physical Chemistry C*. 2009;113(36):15792-5. https://doi.org/10.1021/jp906368f
[89] Jeon TH, Choi W, Park H. Photoelectrochemical and photocatalytic behaviors of hematite-decorated titania nanotube arrays: Energy level mismatch versus surface specific reactivity. *The Journal of Physical Chemistry C*. 2011;115(14):7134-42. https://doi.org/10.1021/jp201215t
[90] Mou F, Xu L, Ma H, Guan J, Chen D-r, Wang S. Facile preparation of magnetic γ-Fe_2O_3/TiO_2 Janus hollow bowls with efficient visible-light photocatalytic activities by asymmetric shrinkage. *Nanoscale*. 2012;4(15):4650-7. https://doi.org/10.1039/C2NR30733B
[91] King LA, Zhao W, Chhowalla M, Riley DJ, Eda G. Photoelectrochemical properties of chemically exfoliated MoS_2. *Journal of Materials Chemistry A*. 2013;1(31):8935-41. https://doi.org/10.1039/C3TA11633F
[92] Zhou W, Yin Z, Du Y, Huang X, Zeng Z, Fan Z, et al. Synthesis of few-layer MoS_2 nanosheet-coated TiO_2 nanobelt heterostructures for enhanced photocatalytic activities. *Small*. 2013;9(1):140-7. https://doi.org/10.1002/smll.201201161
[93] Hu Y, Li D, Zheng Y, Chen W, He Y, Shao Y, et al. $BiVO_4$/TiO_2 nanocrystalline heterostructure: a wide spectrum responsive photocatalyst towards the highly efficient decomposition of gaseous benzene. *Applied Catalysis B: Environmental*. 2011;104(1-2):30-6. https://doi.org/10.1016/j.apcatb.2011.02.031
[94] Scanlon DO, Dunnill CW, Buckeridge J, Shevlin SA, Logsdail AJ, Woodley SM, et al. Band alignment of rutile and anatase TiO_2. *Nature materials*. 2013;12(9):798-801. https://doi.org/10.1038/nmat3697
[95] Kawahara T, Konishi Y, Tada H, Tohge N, Nishii J, Ito S. A patterned TiO_2 (anatase)/TiO_2 (rutile) bilayer-type photocatalyst: effect of the anatase/rutile junction on the photocatalytic activity. *Angewandte Chemie*. 2002;114(15):2935-7. https://doi.org/10.1002/1521-3773(20020802)41:15<2811::AID-ANIE2811>3.0.CO;2-%23

[96] Law M, Greene LE, Radenovic A, Kuykendall T, Liphardt J, Yang P. ZnO− Al_2O_3 and ZnO− TiO_2 core−shell nanowire dye-sensitized solar cells. *The Journal of Physical Chemistry B*. 2006;110(45):22652-63. https://doi.org/10.1021/jp0648644
[97] Wu L, Xing J, Hou Y, Xiao FY, Li Z, Yang HG. Fabrication of regular ZnO/TiO_2 heterojunctions with enhanced photocatalytic properties. *Chemistry–A European Journal*. 2013;19(26):8393-6. https://doi.org/10.1002/chem.201300849
[98] Siedl N, Baumann SO, Elser MJ, Diwald O. Particle networks from powder mixtures: generation of TiO_2–SnO_2 heterojunctions via surface charge-induced heteroaggregation. *The Journal of Physical Chemistry C*. 2012;116(43):22967-73. 10.1021/jp307737s
[99] Kim S, Cho D-H, Chang H-K, Lee H-N, Kim H-J, Park TJ, et al. Selective photoactive gas detection of CO and HCHO using highly porous SnO_2 and SnO_2@ TiO_2 heterostructure. *Sensors and Actuators B: Chemical*. 2022;358:131486. https://doi.org/10.1016/j.snb.2022.131486
[100] Yu H, Liu R, Wang X, Wang P, Yu J. Enhanced visible-light photocatalytic activity of Bi_2WO_6 nanoparticles by Ag_2O cocatalyst. *Applied Catalysis B: Environmental*. 2012;111:326-33. https://doi.org/10.1016/j.apcatb.2011.10.015
[101] Helaïli N, Bessekhouad Y, Bouguelia A, Trari M. Visible light degradation of Orange II using xCuyOz/TiO_2 heterojunctions. *Journal of Hazardous materials*. 2009;168(1):484-92. 10.1016/j.jhazmat.2009.02.066
[102] Bessekhouad Y, Robert D, Weber J-V. Photocatalytic activity of Cu_2O/TiO_2, Bi_2O_3/TiO_2 and $ZnMn_2O_4$/TiO_2 heterojunctions. *Catalysis Today*. 2005;101(3-4):315-21. https://doi.org/10.1016/j.cattod.2005.03.038
[103] Zhang J, Zhu H, Zheng S, Pan F, Wang T. TiO_2 film/Cu_2O microgrid heterojunction with photocatalytic activity under solar light irradiation. *ACS Applied Materials & Interfaces*. 2009;1(10):2111-4. https://doi.org/10.1021/am900463g
[104] Yang L, Luo S, Li Y, Xiao Y, Kang Q, Cai Q. High efficient photocatalytic degradation of p-nitrophenol on a unique Cu_2O/TiO_2 pn heterojunction network catalyst. *Environmental science & technology*. 2010;44(19):7641-6. 10.1021/es101711k
[105] Liu C, Yang Y, Li J, Chen S, Li W, Tang X. An in situ transformation approach for fabrication of $BiVO_4$/WO_3 heterojunction photoanode with high photoelectrochemical activity. *Chemical Engineering Journal*. 2017;326:603-11. https://doi.org/10.1016/j.cej.2017.05.179
[106] Coelho D, Gaudêncio JPR, Carminati SA, Ribeiro FW, Nogueira AF, Mascaro LH. Bi electrodeposition on WO_3 photoanode to improve the photoactivity of the WO_3/$BiVO_4$ heterostructure to water splitting. *Chemical Engineering Journal*. 2020;399:125836:1-11. https://doi.org/10.1016/j.cej.2020.125836
[107] Chen B, Zhang Z, Baek M, Kim S, Kim W, Yong K. An antenna/spacer/reflector based Au/$BiVO_4$/WO_3/Au nanopatterned photoanode for plasmon-enhanced photoelectrochemical water splitting. *Applied Catalysis B: Environmental*. 2018;237:763-771. https://doi.org/10.1016/j.apcatb.2018.06.048
[108] Jeong HW, Jeon TH, Jang JS, Choi W, Park H. Strategic modification of $BiVO_4$ for improving photoelectrochemical water oxidation performance. *The Journal of Physical Chemistry C*. 2013;117(18):9104-9112. https://doi.org/10.1021/jp400415m
[109] Han S, Yu L, Zhang H, Chu Z, Chen X, Xi H, et al. Gold plasmon‐enhanced solar hydrogen production over $SrTiO_3$/TiO_2 heterostructures. *ChemCatChem*. 2019;11(24):6203-6207. https://doi.org/10.1002/cctc.201901399
[110] Wysmulek K, Sar J, Osewski P, Orlinski K, Kolodziejak K, Trenczek-Zajac A, et al. A $SrTiO_3$-TiO_2 eutectic composite as a stable photoanode material for photoelectrochemical hydrogen production. *Applied Catalysis B: Environmental*. 2017;206:538-546. https://doi.org/10.1016/j.apcatb.2017.01.054
[111] Li J, Chen J, Fang H, Guo X, Rui Z. Plasmonic metal bridge leading Type III heterojunctions to robust Type B photothermocatalysts. *Industrial & Engineering Chemistry Research*. 2021;60(23):8420-8429. https://doi.org/10.1021/acs.iecr.1c01198
[112] Li J, Yang X, Ma C, Lei Y, Cheng Z, Rui Z. Selectively recombining the photoinduced charges in bandgap-broken Ag_3PO_4/$GdCrO_3$ with a plasmonic Ag bridge for efficient photothermocatalytic VOCs degradation and CO_2 reduction. *Applied Catalysis B: Environmental*. 2021;291:120053:1-10. https://doi.org/10.1016/j.apcatb.2021.120053
[113] Li J, Feng J, Guo X, Fang H, Chen J, Ma C, et al. Defect-band bridge photothermally activates Type III heterojunction for CO_2 reduction and typical VOCs oxidation. *Applied Catalysis B: Environmental*. 2022;309:121248:1-9. https://doi.org/10.1016/j.apcatb.2022.121248
[114] Chen CY, Shik A, Pitanti A, Tredicucci A, Ercolani D, Sorba L, et al. Electron beam induced current in InSb-InAs nanowire type-III heterostructures. *Applied Physics Letters*. 2012;101(6):063116:1-3. https://doi.org/10.1063/1.4745603
[115] Lee Y, Hwang Y, Chung Y-C. Achieving Type I, II, and III heterojunctions using functionalized MXene. *ACS Applied Materials & Interfaces*. 2015;7(13):7163-7169. https://doi.org/10.1021/acsami.5b00063

[116] Heng H, Gan Q, Meng P, Liu X. The visible-light-driven Type III heterojunction $H_3PW_{12}O_{40}/TiO_2$-In_2S_3: A photocatalysis composite with enhanced photocatalytic activity. *Journal of Alloys and Compounds*. 2017;696:51-9. https://doi.org/10.1016/j.jallcom.2016.11.116
[117] Piña-Pérez Y, Aguilar-Martínez O, Acevedo-Peña P, Santolalla-Vargas C, Oros-Ruíz S, Galindo-Hernández F, et al. Novel ZnS-ZnO composite synthesized by the solvothermal method through the partial sulfidation of ZnO for H_2 production without sacrificial agent. *Applied Catalysis B: Environmental*. 2018;230:125-34. https://doi.org/10.1016/j.apcatb.2018.02.047
[118] Luan Q, Chen Q, Zheng J, Guan R, Fang Y, Hu X. Construction of 2D-ZnS@ ZnO Z-scheme heterostructured nanosheets with a highly ordered ZnO core and disordered ZnS shell for enhancing photocatalytic hydrogen evolution. *ChemNanoMat*. 2020;6(3):470-9. https://doi.org/10.1002/cnma.201900630
[119] Chen HM, Chen CK, Liu RS, Wu CC, Chang WS, Chen KH, et al. A new approach to solar hydrogen production: a ZnO–ZnS solid solution nanowire array photoanode. *Advanced Energy Materials*. 2011;1(5):742-7. https://doi.org/10.1002/aenm.201100246
[120] Low J, Jiang C, Cheng B, Wageh S, Al-Ghamdi AA, Yu J. A Review of direct Z-scheme photocatalysts. *Small Methods*. 2017;1(5):1700080. https://doi.org/10.1002/smtd.201700080
[121] Sun Q, Lv K, Zhang Z, Li M, Li B. Effect of contact interface between TiO_2 and g-C_3N_4 on the photoreactivity of g-C_3N_4/TiO_2 photocatalyst:(0 0 1) vs (1 0 1) facets of TiO_2. *Applied Catalysis B: Environmental*. 2015;164:420-7. https://doi.org/10.1016/j.apcatb.2014.09.043
[122] Meng A, Zhu B, Zhong B, Zhang L, Cheng B. Direct z-scheme TiO_2/CdS hierarchical photocatalyst for enhanced photocatalytic H_2-production activity. *Applied Surface Science*. 2017;422:518-27. https://doi.org/10.1016/j.apsusc.2017.06.028
[123] Ma K, Yehezkeli O, Domaille DW, Funke HH, Cha JN. Enhanced hydrogen production from DNA-assembled Z-scheme TiO_2–CdS photocatalyst systems. *Angewandte Chemie International Edition*. 2015;54(39):11490-4. https://doi.org/10.1002/anie.201504155
[124] Wang S, Zhu B, Liu M, Zhang L, Yu J, Zhou M. Direct Z-scheme ZnO/CdS hierarchical photocatalyst for enhanced photocatalytic H_2-production activity. *Applied Catalysis B: Environmental*. 2019;243:19-26. https://doi.org/10.1016/j.apcatb.2018.10.019
[125] QingáLu G. Enhanced photocatalytic hydrogen evolution by prolonging the lifetime of carriers in ZnO/CdS heterostructures. *Chemical Communications*. 2009(23):3452-4. https://doi.org/10.1039/B904668B
[126] Nie N, Zhang L, Fu J, Cheng B, Yu J. Self-assembled hierarchical direct Z-scheme g-C_3N_4/ZnO microspheres with enhanced photocatalytic CO_2 reduction performance. *Applied Surface Science*. 2018;441:12-22. https://doi.org/10.1016/j.apsusc.2018.01.193
[127] Li N, Tian Y, Zhao J, Zhang J, Zuo W, Kong L, et al. Z-scheme 2D/3D g-C3N4@ ZnO with enhanced photocatalytic activity for cephalexin oxidation under solar light. *Chemical Engineering Journal*. 2018;352:412-22. https://doi.org/10.1016/j.cej.2018.07.038
[128] Zhang P, Zhang L, Dong E, Zhang X, Zhang W, Wang Q, et al. Synthesis of $CaIn_2S_4/TiO_2$ heterostructures for enhanced UV–visible light photocatalytic activity. *Journal of Alloys and Compounds*. 2021;885:161027. https://doi.org/10.1016/j.jallcom.2021.161027
[129] Di T, Xu Q, Ho W, Tang H, Xiang Q, Yu J. Review on metal sulphide-based Z-scheme photocatalysts. *ChemCatChem*. 2019;11(5):1394-411. https://doi.org/10.1002/cctc.201802024
[130] Nguyen NT, Altomare M, Yoo JE, Taccardi N, Schmuki P. Noble metals on anodic TiO_2 nanotube mouths: Thermal dewetting of minimal Pt Co-catalyst loading leads to significantly enhanced photocatalytic H_2 generation. *Advanced Energy Materials*. 2016;6(2):1501926. https://doi.org/10.1002/aenm.201501926
[131] Murthy DH, Matsuzaki H, Wang Q, Suzuki Y, Seki K, Hisatomi T, et al. Revealing the role of the Rh valence state, La doping level and Ru cocatalyst in determining the H_2 evolution efficiency in doped $SrTiO_3$ photocatalysts. *Sustainable Energy & Fuels*. 2019;3(1):208-18. https://doi.org/10.1039/C8SE00487K
[132] Su R, Tiruvalam R, Logsdail AJ, He Q, Downing CA, Jensen MT, et al. Designer titania-supported Au–Pd nanoparticles for efficient photocatalytic hydrogen production. *ACS Nano*. 2014;8(4):3490-7. https://doi.org/10.1021/nn500963m
[133] Rej S, Hejazi SMH, Badura Z, Zoppellaro G, Kalytchuk S, Kment Š, et al. Light-induced defect formation and Pt single atoms synergistically boost photocatalytic H_2 production in 2D TiO_2-bronze nanosheets. *ACS Sustainable Chemistry & Engineering*. 2022;10(51):17286-96. https://doi.org/10.1021/acssuschemeng.2c05708
[134] Shen R, Xie J, Xiang Q, Chen X, Jiang J, Li X. Ni-based photocatalytic H_2-production cocatalysts2. *Chinese Journal of Catalysis*. 2019;40(3):240-88. https://doi.org/10.1016/S1872-2067(19)63294-8

[135] Ren X, Wei S, Wang Q, Shi L, Wang X-S, Wei Y, et al. Rational construction of dual cobalt active species encapsulated by ultrathin carbon matrix from MOF for boosting photocatalytic H_2 generation. *Applied Catalysis B: Environmental*. 2021;286:119924. https://doi.org/10.1016/j.apcatb.2021.119924
[136] Xiao S, Liu P, Zhu W, Li G, Zhang D, Li H. Copper nanowires: a substitute for noble metals to enhance photocatalytic H_2 generation. *Nano Letters*. 2015;15(8):4853-8. https://doi.org/10.1021/acs.nanolett.5b00082
[137] Lee B-H, Park S, Kim M, Sinha AK, Lee SC, Jung E, et al. Reversible and cooperative photoactivation of single-atom Cu/TiO_2 photocatalysts. *Nature materials*. 2019;18(6):620-6. 10.1038/s41563-019-0344-1
[138] Ran J, Zhang J, Yu J, Jaroniec M, Qiao SZ. Earth-abundant cocatalysts for semiconductor-based photocatalytic water splitting. *Chemical Society Reviews*. 2014;43(22):7787-812. https://doi.org/10.1039/C3CS60425J
[139] Takata T, Jiang J, Sakata Y, Nakabayashi M, Shibata N, Nandal V, et al. Photocatalytic water splitting with a quantum efficiency of almost unity. *Nature*. 2020;581(7809):411-414. https://doi.org/10.1038/s41586-020-2278-9
[140] Li X, Zhao L, Yu J, Liu X, Zhang X, Liu H, et al. Water splitting: from electrode to green energy system. *Nano-Micro Letters*. 2020;12(1):131. 1-29. https://doi.org/10.1007/s40820-020-00469-3
[141] You B, Sun Y. Innovative strategies for electrocatalytic water splitting. *Accounts of Chemical Research*. 2018;51(7):1571-1580. https://doi.org/10.1021/acs.accounts.8b00002
[142] Anantharaj S, Karthick K, Venkatesh M, Simha TV, Salunke AS, Ma L, et al. Enhancing electrocatalytic total water splitting at few layer Pt-NiFe layered double hydroxide interfaces. *Nano Energy*. 2017;39:30-43. https://doi.org/10.1016/j.nanoen.2017.06.027
[143] You B, Liu X, Hu G, Gul S, Yano J, Jiang D-e, et al. Universal surface engineering of transition metals for superior electrocatalytic hydrogen evolution in neutral water. *Journal of the American Chemical Society*. 2017;139(35):12283-90. https://doi.org/10.1021/jacs.7b06434
[144] Peng J, Dong W, Wang Z, Meng Y, Liu W, Song P, et al. Recent advances in 2D transition metal compounds for electrocatalytic full water splitting in neutral media. *Materials today advances*. 2020;8:100081. https://doi.org/10.1016/j.mtadv.2020.100081
[145] Zhou Z, Pei Z, Wei L, Zhao S, Jian X, Chen Y. Electrocatalytic hydrogen evolution under neutral pH conditions: current understandings, recent advances, and future prospects. *Energy & Environmental Science*. 2020;13(10):3185-206. https://doi.org/10.1039/D0EE01856B
[146] Yin H, Zhao S, Zhao K, Muqsit A, Tang H, Chang L, et al. Ultrathin platinum nanowires grown on single-layered nickel hydroxide with high hydrogen evolution activity. *Nature Communications*. 2015;6(1):1-8. 10.1038/ncomms7430
[147] Lu B, Guo L, Wu F, Peng Y, Lu JE, Smart TJ, et al. Ruthenium atomically dispersed in carbon outperforms platinum toward hydrogen evolution in alkaline media. *Nature Communications*. 2019;10(1):1-11. https://doi.org/10.1038/s41467-019-08419-3
[148] Wang P, Zhang X, Zhang J, Wan S, Guo S, Lu G, et al. Precise tuning in platinum-nickel/nickel sulfide interface nanowires for synergistic hydrogen evolution catalysis. *Nature Communications*. 2017;8(1):1-9. https://doi.org/10.1038/ncomms14580
[149] Chen J, Chen C, Qin M, Li B, Lin B, Mao Q, et al. Reversible hydrogen spillover in Ru-WO_{3-x} enhances hydrogen evolution activity in neutral pH water splitting. *Nature Communications*. 2022;13(1):5382. 10.1038/s41467-022-33007-3
[150] Jiang N, You B, Sheng M, Sun Y. Electrodeposited cobalt-phosphorous-derived films as competent bifunctional catalysts for overall water splitting. *Angewandte Chemie International Edition*. 2015; 127:6349-6352. https://doi.org/10.1002/ange.201501616
[151] You B, Jiang N, Sheng M, Bhushan MW, Sun Y. Hierarchically porous urchin-Like Ni_2P superstructures supported on nickel foam as efficient bifunctional electrocatalysts for overall water splitting. *ACS Catalysis*. 2016;6(2):714-21. https://doi.org/10.1021/acscatal.5b02193
[152] You B, Jiang N, Sheng M, Gul S, Yano J, Sun Y. High-performance overall water splitting electrocatalysts derived from Cobalt-based metal–organic frameworks. *Chemistry of Materials*. 2015;27(22):7636-42. https://doi.org/10.1021/acs.chemmater.5b02877
[153] You B, Sun Y. Hierarchically porous nickel sulfide multifunctional superstructures. *Advanced Energy Materials*. 2016;6(7):1502333. https://doi.org/10.1002/aenm.201502333
[154] Rausch B, Symes MD, Chisholm G, Cronin L. Decoupled catalytic hydrogen evolution from a molecular metal oxide redox mediator in water splitting. *Science*. 2014;345(6202):1326-30. 10.1126/science.1257443
[155] Symes MD, Cronin L. Decoupling hydrogen and oxygen evolution during electrolytic water splitting using an electron-coupled-proton buffer. *Nature chemistry*. 2013;5(5):403-9. https://doi.org/10.1038/nchem.1621

[156] Rausch B, Symes MD, Cronin L. A bio-inspired, small molecule electron-coupled-proton buffer for decoupling the half-reactions of electrolytic water splitting. *Journal of the American Chemical Society*. 2013;135(37):13656-9. https://doi.org/10.1021/ja4071893
[157] Li W, Jiang N, Hu B, Liu X, Song F, Han G, et al. Electrolyzer design for flexible decoupled water splitting and organic upgrading with electron reservoirs. *Chem*. 2018;4(3):637-49. https://doi.org/10.1016/j.chempr.2017.12.019
[158] Chen L, Dong X, Wang Y, Xia Y. Separating hydrogen and oxygen evolution in alkaline water electrolysis using nickel hydroxide. *Nature Communications*. 2016;7(1):1-8. https://doi.org/10.1038/ncomms11741
[159] Landman A, Dotan H, Shter GE, Wullenkord M, Houaijia A, Maljusch A, et al. Photoelectrochemical water splitting in separate oxygen and hydrogen cells. *Nature Materials*. 2017;16(6):646-51. https://doi.org/10.1038/nmat4876
[160] You B, Jiang N, Liu X, Sun Y. Simultaneous H_2 generation and biomass upgrading in water by an efficient noble-metal-free bifunctional electrocatalyst. *Angewandte Chemie International Edition*. 2016;55(34):9913-7. https://doi.org/10.1002/anie.201603798
[161] Chaplin BP. The prospect of electrochemical technologies advancing worldwide water treatment. *Accounts of Chemical Research*. 2019;52(3):596-604. https://doi.org/10.1021/acs.accounts.8b00611
[162] Du L, Sun Y, You B. Hybrid water electrolysis: Replacing oxygen evolution reaction for energy-efficient hydrogen production and beyond. *Materials Reports: Energy*. 2021;1(1):100004:1-14. https://doi.org/10.1016/j.matre.2020.12.001
[163] Suzuki N, Okazaki A, Kuriyama H, Serizawa I, Hirami Y, Hara A, et al. Synergetic effect in water treatment with mesoporous TiO_2/BDD hybrid electrode. *RSC Advances*. 2020;10(3):1793-8. https://doi.org/10.1039/C9RA10318J
[164] Garcia-Segura S, Nienhauser AB, Fajardo AS, Bansal R, Conrad CL, Fortner JD, et al. Disparities between experimental and environmental conditions: Research steps toward making electrochemical water treatment a reality. *Current Opinion in Electrochemistry*. 2020;22:9-16. https://doi.org/10.1016/j.coelec.2020.03.001
[165] Nichols EM, Gallagher JJ, Liu C, Su Y, Resasco J, Yu Y, et al. Hybrid bioinorganic approach to solar-to-chemical conversion. *Proceedings of the National Academy of Sciences*. 2015;112(37):11461-11466. 10.1073/pnas.1508075112
[166] Wang A-L, Xu H, Li G-R. NiCoFe Layered Triple Hydroxides with Porous Structures as High-Performance Electrocatalysts for Overall Water Splitting. *ACS Energy Letters*. 2016;1(2):445-53. https://doi.org/10.1021/acsenergylett.6b00219
[167] Hwang J, Rao RR, Giordano L, Katayama Y, Yu Y, Shao-Horn Y. Perovskites in catalysis and electrocatalysis. *Science*. 2017;358(6364):751-756. https://doi.org/10.1126/science.aam709
[168] Priya P, Aluru N. Accelerated design and discovery of perovskites with high conductivity for energy applications through machine learning. *npj Computational Materials*. 2021;7(1):1-12. https://doi.org/10.1038/s41524-021-00551-3
[169] Li Z, Achenie LE, Xin H. An adaptive machine learning strategy for accelerating discovery of perovskite electrocatalysts. *ACS Catalysis*. 2020;10(7):4377-4384. https://doi.org/10.1021/acscatal.9b05248
[170] Mefford JT, Rong X, Abakumov AM, Hardin WG, Dai S, Kolpak AM, et al. Water electrolysis on $La_{1-x}Sr_x CoO_{3-\delta}$ perovskite electrocatalysts. *Nature Communications*. 2016;7(1):11053:1-11. https://doi.org/10.1038/ncomms11053
[171] Liang X, Shi L, Liu Y, Chen H, Si R, Yan W, et al. Activating inert, nonprecious perovskites with iridium dopants for efficient oxygen evolution reaction under acidic conditions. *Angewandte Chemie International Edition*. 2019;58(23):7631-7635. https://doi.org/10.1002/anie.201900796
[172] Thanh TD, Chuong ND, Balamurugan J, Van Hien H, Kim NH, Lee JH. Porous hollow-structured $LaNiO_3$ stabilized N, S-codoped graphene as an active electrocatalyst for oxygen reduction reaction. *Small*. 2017;13(39):1701884:1-11. https://doi.org/10.1002/smll.201701884
[173] Li Y, Zhang X, Wu Z, Sheng H, Li C, Li H, et al. Coupling porous Ni doped $LaFeO_3$ nanoparticles with amorphous FeOOH nanosheets yields an interfacial electrocatalyst for electrocatalytic oxygen evolution. *Journal of Materials Chemistry A*. 2021;9(41):23545-23554. https://doi.org/10.1039/D1TA05777D
[174] Ji Q, Bi L, Zhang J, Cao H, Zhao XS. The role of oxygen vacancies of ABO_3 perovskite oxides in the oxygen reduction reaction. *Energy & Environmental Science*. 2020;13(5):1408-1428. https://doi.org/10.1039/D0EE00092B
[175] Guan D, Zhou J, Huang Y-C, Dong C-L, Wang J-Q, Zhou W, et al. Screening highly active perovskites for hydrogen-evolving reaction via unifying ionic electronegativity descriptor. *Nature Communications*. 2019;10(1):1-8. https://doi.org/10.1038/s41467-019-11847-w
[176] Chen H, Lim C, Zhou M, He Z, Sun X, Li X, et al. Activating lattice oxygen in perovskite oxide by B-site cation doping for modulated stability and activity at elevated temperatures. *Advanced Science*. 2021;8(22):2102713:1-11. https://doi.org/10.1002/advs.202102713

[177] Bu Y, Jang H, Gwon O, Kim SH, Joo SH, Nam G, et al. Synergistic interaction of perovskite oxides and N-doped graphene in versatile electrocatalyst. *Journal of Materials Chemistry A*. 2019;7(5):2048-2054. https://doi.org/10.1039/C8TA09919G
[178] Yu L, Zhu Q, Song S, McElhenny B, Wang D, Wu C, et al. Non-noble metal-nitride based electrocatalysts for high-performance alkaline seawater electrolysis. *Nature Communications*. 2019;10(1):5106:1-10. https://doi.org/10.1038/s41467-019-13092-7
[179] Sun F, Qin J, Wang Z, Yu M, Wu X, Sun X, et al. Energy-saving hydrogen production by chlorine-free hybrid seawater splitting coupling hydrazine degradation. *Nature Communications*. 2021;12(1):4182:1-11. https://doi.org/10.1038/s41467-021-24529-3
[180] Ahmad NA, Goh PS, Yogarathinam LT, Zulhairun AK, Ismail AF. Current advances in membrane technologies for produced water desalination. *Desalination*. 2020;493:114643:1-22. https://doi.org/10.1016/j.desal.2020.114643
[181] Generous MM, Qasem NAA, Akbar UA, Zubair SM. Techno-economic assessment of electrodialysis and reverse osmosis desalination plants. *Separation and Purification Technology*. 2021;272:118875:1-22. https://doi.org/10.1016/j.seppur.2021.118875
[182] Xie H, Zhao Z, Liu T, Wu Y, Lan C, Jiang W, et al. A membrane-based seawater electrolyser for hydrogen generation. *Nature*. 2022;612(7941):673-8. https://doi.org/10.1038/s41586-022-05379-5
[183] Hisatomi T, Kubota J, Domen K. Recent advances in semiconductors for photocatalytic and photoelectrochemical water splitting. *Chemical Society Reviews*. 2014;43(22):7520-35. https://doi.org/10.1039/C3CS60378D
[184] Zhang T, Qian Y, Gao H, Huang-Fu Z-C, Brown JB, Rao Y. Surface states for photoelectrodes of gallium phosphide (GaP) with surface-specific electronic spectra and phase measurements. *The Journal of Physical Chemistry C*. 2022;126(15):6761-72. https://doi.org/10.1021/acs.jpcc.2c00412
[185] Narangari PR, Butson JD, Tan HH, Jagadish C, Karuturi S. Surface-tailored InP nanowires via self-assembled Au nanodots for efficient and stable photoelectrochemical hydrogen evolution. *Nano Letters*. 2021;21(16):6967-74. 10.1021/acs.nanolett.1c02205
[186] Ben-Naim M, Aldridge CW, Steiner MA, Britto RJ, Nielander AC, King LA, et al. Engineering surface architectures for improved durability in III–V photocathodes. *ACS Applied Materials & Interfaces*. 2022;14(18):20385-92. https://doi.org/10.1021/acsami.1c18938
[187] Dong WJ, Xiao Y, Yang KR, Ye Z, Zhou P, Navid IA, et al. Pt nanoclusters on GaN nanowires for solar-asssisted seawater hydrogen evolution. *Nature Communications*. 2023;14(1):179. 10.1038/s41467-023-35782-z
[188] Balocchi A, Da Gama Fernandes Vieira L, Formiga Franklin G, Taberna P-L, Barnabe A, Vedrenne M, et al. Controlling 2D/2D contacts in 2D TMDC nanostructured films for solar-to-hydrogen conversion. *ACS Applied Energy Materials*. 2023. https://doi.org/10.1021/acsaem.2c02921
[189] Cheng Y, Xiao C, Mahmoudi B, Scheer R, Maijenburg AW, Osterloh FE. Effect of charge selective contacts on the quasi Fermi level splitting of $CuGa_3Se_5$ thin film photocathodes for hydrogen evolution and methylviologen reduction. *EES Catalysis*. 2023. https://doi.org/10.1039/D2EY00062H
[190] Qin C, Chen X, Jiang N, Liang R, Li Z, Zheng Z, et al. Surface densification strategy assisted efficient Cu_2O heterojunction photocathode for solar water splitting. *Materials Today Nano*. 2023;21:100294. https://doi.org/10.1016/j.mtnano.2022.100294
[191] Ida S, Yamada K, Matsunaga T, Hagiwara H, Matsumoto Y, Ishihara T. Preparation of p-Type $CaFe_2O_4$ photocathodes for producing hydrogen from water. *Journal of the American Chemical Society*. 2010;132(49):17343-5. https://doi.org/10.1021/ja106930f
[192] Yuan Y, Zhong B, Li F, Wu H, Liu J, Yang H, et al. Surface phosphorization for the enhanced photoelectrochemical performance of an Fe_2O_3/Si photocathode. *Nanoscale*. 2022;14(31):11261-9. https://doi.org/10.1039/D2NR02693G
[193] Han Y, Wang J, Wang X, Wu Z, Zhao Y, Huang H, et al. An in-situ transient photo-induced voltage method to understand the PEC efficiency of C, N co-doped TiO_2 photoanode. *Applied Surface Science*. 2023;608:155282. https://doi.org/10.1016/j.apsusc.2022.155282
[194] Shao C, Malik AS, Han J, Li D, Dupuis M, Zong X, et al. Oxygen vacancy engineering with flame heating approach towards enhanced photoelectrochemical water oxidation on WO_3 photoanode. *Nano Energy*. 2020;77:105190. https://doi.org/10.1016/j.nanoen.2020.105190
[195] Sharma P, Jang JW, Lee JS. Key strategies to advance the photoelectrochemical water splitting performance of α-Fe_2O_3 photoanode. *ChemCatChem*. 2019;11(1):157-79. https://doi.org/10.1002/cctc.201801187
[196] Kim JH, Lee JS. Elaborately modified $BiVO_4$ photoanodes for solar water splitting. *Advanced Materials*. 2019;31(20):1806938. https://doi.org/10.1002/adma.201806938
[197] Doiphode V, Vairale P, Sharma V, Waghmare A, Punde A, Shinde P, et al. Solution-processed electrochemical synthesis of $ZnFe_2O_4$ photoanode for photoelectrochemical water splitting. *Journal of Solid State Electrochemistry*. 2021;25(6):1835-46. https://doi.org/10.1007/s10008-021-04953-7

[198] Li Y, Zhang N, Liu C, Zhang Y, Xu X, Wang W, et al. Metastable-phase β-Fe_2O_3 photoanodes for solar water splitting with durability exceeding 100 h. *Chinese Journal of Catalysis*. 2021;42(11):1992-8. https://doi.org/10.1016/S1872-2067(21)63822-6
[199] Li F, Jian J, Xu Y, Liu W, Ye Q, Feng F, et al. Surface defect passivation of Ta_3N_5 photoanode via pyridine grafting for enhanced photoelectrochemical performance. *The Journal of Chemical Physics*. 2020;153(2):024705. https://doi.org/10.1063/5.0012873
[200] Higashi M, Kato Y, Iwase Y, Tomita O, Abe R. RhO_x cocatalyst for efficient water oxidation over TaON photoanodes in wide pH range under visible-light irradiation. *Journal of Photochemistry and Photobiology A: Chemistry*. 2021;419:113463. https://doi.org/10.1016/j.jphotochem.2021.113463
[201] Ma Z, Thersleff T, Görne AL, Cordes N, Liu Y, Jakobi S, et al. Quaternary core–shell oxynitride nanowire photoanode containing a hole-extraction gradient for photoelectrochemical water oxidation. *ACS Applied Materials & Interfaces*. 2019;11(21):19077-86. 10.1021/acsami.9b02483
[202] Li Y, Takata T, Cha D, Takanabe K, Minegishi T, Kubota J, et al. Vertically aligned Ta_3N_5 nanorod arrays for solar-driven photoelectrochemical water splitting. *Advanced Materials*. 2013;25(1):125-31. https://doi.org/10.1002/adma.201202582
[203] Hara M, Chiba E, Ishikawa A, Takata T, Kondo JN, Domen K. Ta_3N_5 and TaON thin films on Ta foil: surface composition and stability. *The Journal of Physical Chemistry B*. 2003;107(48):13441-5. 10.1021/jp036189t
[204] Chun W-J, Ishikawa A, Fujisawa H, Takata T, Kondo JN, Hara M, et al. Conduction and valence band positions of Ta_2O_5, TaON, and Ta_3N_5 by UPS and electrochemical methods. *The Journal of Physical Chemistry B*. 2003;107(8):1798-803. 10.1021/jp027593f
[205] International Energy Agency (IEA), *Global hydrogen demand by sector in the sustainable development scenario*, 2019-2070, Paris https://www.iea.org/data-and-statistics/charts/global-hydrogen-demand-by-sector-in-the-sustainable-development-scenario-2019-2070, IEA. License: CC BY 4.0. 2022. [Accessed date: 01 December 2022].
[206] The New Energy and Industrial Technology Development Organization (NEDO), *The world's largest-class hydrogen production, Fukushima Hydrogen Energy Research Field (FH_2R) now is completed at Namie town in Fukushima.* 2020. https://www.nedo.go.jp/english/news/AA5en_100422.html [Accessed date: 01 December 2022].
[207] The New Energy and Industrial Technology Development Organization (NEDO), *Japan policy and activity on hydrogen energy.* 2019. https://www.nedo.go.jp/content/100890039.pdf [Accessed date: 01 December 2022].
[208] Renew Economy, *Denmark plans massive "energy islands" to deliver 4GW of green fuel to economy*. 2020. https://reneweconomy.com.au/denmark-plans-massive-energy-islands-to-deliver-4gw-of-green-fuel-to-economy-25361/amp/ [Accessed date: 01 December 2022]
[209] Renew Economy, *German steel giant Thyssenkrupp plans 500MW green hydrogen plant.* 2021. https://reneweconomy.com.au/german-steel-giant-thyssenkrupp-plans-500mw-green-hydrogen-plant/amp/[Accessed date: 01 December 2022].
[210] Renew Economy, *CWP joins global initiative targeting 25GW of green hydrogen by 2026*. 2020. https://reneweconomy.com.au/cwp-joins-global-initiative-targeting-25gw-of-green-hydrogen-by-2026/amp/[Accessed date: 01 December 2022].
[211] Renew Economy, Bill Gates backs $1/kg green hydrogen water splitter technology. 2021. https://reneweconomy-com-au.cdn.ampproject.org/c/s/reneweconomy.com.au/bill-gates-backs-1-kg-green-hydrogen-water-splitter-technology/amp/?fbclid=IwAR06S41pYLQDUOWvPY9LQN_GF_5RB3XGs6OVqc6hBbJ_LnQTEXCKqtbmG0Q [Accessed date: 01 December 2022].
[212] International Energy Agency (IEA), Fuel cell electric vehicle stock by region, 2017-2020, Paris https://www.iea.org/data-and-statistics/charts/fuel-cell-electric-vehicle-stock-by-region-2017-2020. License: CC BY 4.0. 2022. [Accessed date: 01 December 2022].
[213] Cullen, D.A.; Neyerlin, K.; Ahluwalia, R.K.; Mukundan, R.; More, K.L.; Borup, R.L.; Weber, A.Z.; Myers, D.J.; Kusoglu, A. New roads and challenges for fuel cells in heavy-duty transportation. *Nature Energy* 2021, 6, 462-474. https://doi.org/10.1038/s41560-021-00775-z
[214] International Energy Agency (IEA), Fuel cell electric vehicle stock by region and by mode, 2021, Paris https://www.iea.org/data-and-statistics/charts/fuel-cell-electric-vehicle-stock-by-region-and-by-mode-2021. License: CC BY 4.0. 2022. [Accessed date: 01 December 2022].
[215] Khan U, Yamamoto T, Sato H. Understanding the discontinuance trend of hydrogen fuel cell vehicles in Japan. *International Journal of Hydrogen Energy*. 2022;47(75):31949-63. https://doi.org/10.1016/j.ijhydene.2022.07.141
[216] ABC News, Are hydrogen fuel cell vehicles the future of autos?. https://abcnews.go.com/Business/hydrogen-fuel-cell-vehicles-future-autos/story?id=74583475 [Accessed date: 01 December 2022] doi:https://abcnews.go.com/Business/hydrogen-fuel-cell-vehicles-future-autos/story?id=74583475.

[217] HyundaiMotorGroup, Popularizing FCEVs: NEXO sales over 10,000 Units. 2020. https://tech.hyundaimotorgroup.com/article/popularizing-fcevs-nexo-sales-over-10000-units/#:~:text=Hyundai%20Motor%20Company%20has%20succeeded,exceeded%2010%2C000%20units%20in%20Korea. [Accessed date: 01 December 2022]